

# Evidence of recent active volcanism in the Balleny Islands (Antarctica) from ice core records

Dieter R Tetzner<sup>1</sup>, Elizabeth Ruth Thomas<sup>1</sup>, Claire S Allen<sup>1</sup>, and Alma Piermattei<sup>2</sup>

<sup>1</sup>British Antarctic Survey

<sup>2</sup>Department of Geography, University of Cambridge

November 23, 2022

## Abstract

Records of active volcanism in Antarctica provide key information to understand the role of volcanoes shaping the polar climate and its potential impacts on the cryosphere. The lack of historical records of volcanic activity in the region has limited our comprehension of Antarctic volcanism. Remote sensing can provide insight into active volcanism during the satellite era, although the evidence is often inconclusive. Here we present a detailed study from multiple Antarctic ice cores to provide independent evidence of active volcanism in the sub-Antarctic Balleny Islands in 2001 AD, supporting un-verified images from satellites. The ice core records reveal elevated inputs of sulphate and microparticles from a local Antarctic volcanic source. In-phase deposition of volcanic products confirmed a rapid tropospheric transport of volcanic emissions from a small-to-moderate, local eruption during 2001. Air mass trajectories demonstrated some air parcels were transported over the West Antarctic Ice sheet from the Balleny Islands to ice core sites at the time of the potential eruption, establishing a route for transport and deposition of volcanic products over the ice sheet. The data presented here validate previous remote sensing observations and confirms a volcanic event in the Balleny Islands during 2001 AD. This newly identified eruption provides a case study of recent Antarctic volcanism and a consistent XXI century chronostratigraphic marker for ice core sites in Marie Byrd Land, Ellsworth Land and the southern Antarctic Peninsula.

1

2 **Evidence of recent active volcanism in the Balleny Islands (Antarctica) from ice core**  
3 **records**

4 **Dieter. R. Tetzner<sup>1,2</sup>, Elizabeth. R. Thomas<sup>1</sup>, Claire. S. Allen<sup>1</sup> and Alma. Piermattei<sup>3</sup>**

5 <sup>1</sup>British Antarctic Survey, Cambridge, United Kingdom. <sup>2</sup>Department of Earth Sciences,  
6 University of Cambridge, Cambridge, United Kingdom. <sup>3</sup>Department of Geography, University  
7 of Cambridge, Cambridge, United Kingdom.

8 Corresponding author: Dieter Tetzner ([dietet95@bas.ac.uk](mailto:dietet95@bas.ac.uk))

9 **Key Points:**

- 10 • Evidence of active volcanism in the sub-Antarctic Balleny Islands in 2001 AD,  
11 supporting un-verified images from satellites.
- 12 • The identification of a 21<sup>st</sup> century volcanic chronostratigraphic marker in ice cores from  
13 the Antarctic Peninsula and West Antarctica.

## 14 **Abstract**

15 Records of active volcanism in Antarctica provide key information to understand the role of  
16 volcanoes shaping the polar climate and its potential impacts on the cryosphere. The lack of  
17 historical records of volcanic activity in the region has limited our comprehension of Antarctic  
18 volcanism. Remote sensing can provide insight into active volcanism during the satellite era,  
19 although the evidence is often inconclusive. Here we present a detailed study from multiple  
20 Antarctic ice cores to provide independent evidence of active volcanism in the sub-Antarctic  
21 Balleny Islands in 2001 AD, supporting un-verified images from satellites. The ice core records  
22 reveal elevated inputs of sulphate and microparticles from a local Antarctic volcanic source. In-  
23 phase deposition of volcanic products confirmed a rapid tropospheric transport of volcanic  
24 emissions from a small-to-moderate, local eruption during 2001. Air mass trajectories  
25 demonstrated some air parcels were transported over the West Antarctic Ice sheet from the  
26 Balleny Islands to ice core sites at the time of the potential eruption, establishing a route for  
27 transport and deposition of volcanic products over the ice sheet. The data presented here validate  
28 previous remote sensing observations and confirms a volcanic event in the Balleny Islands  
29 during 2001 AD. This newly identified eruption provides a case study of recent Antarctic  
30 volcanism and a consistent XXI century chronostratigraphic marker for ice core sites in Marie  
31 Byrd Land, Ellsworth Land and the southern Antarctic Peninsula.

## 32 **1 Introduction**

33 Antarctica is one of the least volcanically active regions in the world, with the highest  
34 number of volcanoes listed as uncertainly active and many others hidden beneath the ice sheet  
35 (Hund, 2014). Over 100 volcanoes have been identified in the Antarctic continent and sub-  
36 Antarctic Islands (LeMasurier et al., 1990; de Vries et al., 2018) with more than twenty  
37 documented in the historical records (Patrick & Smellie, 2013). Among the historically active,  
38 just two are frequently monitored by ground-based instruments (Mount Erebus and Deception  
39 Island) (LeMasurier et al., 1990; Patrick & Smellie, 2013), while the others are rarely surveyed  
40 due to their extreme isolation. Recently, remote sensing techniques have helped to monitor  
41 volcanism through the region. However, high detection thresholds and coarse spatial resolution  
42 have hindered the capacity of some sensors to identify accurately the occurrence of volcanic  
43 activity (Patrick & Smellie, 2013). Moreover, the effects of volcanism can be rapidly obscured in  
44 the Antarctic and sub-Antarctic environment due to frequent snowfall and cloud coverage  
45 (LeMasurier et al., 1990). Even though Antarctic volcanoes do not present significant direct  
46 hazards, their study is important for many areas of research. Mainly, geothermal heat flux  
47 estimates (Vogel et al., 2006), ice flow dynamics models (Bingham & Siegert 2009) and the  
48 volcanic effects on the polar climate (Robock, 2000; Cole-Dai, 2010; Sigl et al., 2014).  
49 Altogether, the remoteness and inaccessibility of most of the Antarctic volcanoes have strongly  
50 limited our knowledge of the Antarctic volcanic activity.

51 An alternative way to study volcanic activity in Antarctica is the analyses of volcanic  
52 tephra (assortment of fragments, from blocks of material to ash, ejected into the air during a  
53 volcanic eruption) (Kittleman, 1979) preserved in ice core layers. Volcanic eruptions emit large  
54 amounts of particulate matter and sulphur compounds into the atmosphere. Sulphur compounds  
55 are oxidized to sulphuric acid ( $\text{H}_2\text{SO}_4^{2-}$ ) and travel as particulate aerosols in the atmosphere.  
56 Volcanic sulphate aerosols and tephra in the atmosphere can be transported thousands of

57 kilometres from the volcanic source, to be deposited and preserved on polar ice sheets (Koffman  
58 et al., 2017). Measurements of sulphate concentrations and electric conductivity (EC) in the ice  
59 strata help to detect and quantify past volcanic activity over thousands of years (Cole-Dai et al.,  
60 1997; Cole-Dai, 2010). Similarly, the physical and chemical characterization of tephra and  
61 cryptotephra (micrometre-sized tephra) embedded in ice layers can record past volcanic activity  
62 and fingerprint the source of the volcanic eruptions (Dunbar & Kurbatov, 2011; Narcisi et al.,  
63 2019). These methods have been applied to several Antarctic ice cores, providing evidence of  
64 past volcanic activity at regional, hemispheric and global scales (Udisti et al., 2000; Basile et al.,  
65 2001; Jiang et al., 2012; Parrenin et al., 2012; Severi et al., 2012; Fujita et al., 2015; Narcisi et  
66 al., 2016; Lee et al., 2019). From a regional perspective, the study of volcanic products preserved  
67 in ice cores has contributed to determining the recurrence of explosive volcanic activity in  
68 different volcanic groups and provinces around Antarctica (Narcisi et al., 2005; Narcisi et al.,  
69 2010; Narcisi et al., 2012).

70 Previous studies have demonstrated that ice cores from the Antarctic Peninsula, Ellsworth  
71 Land and Marie Byrd Land record large-scale and regional explosive volcanic eruptions (Palais,  
72 1985; Cole-Dai et al., 1997; Dunbar et al., 2003; Dixon et al., 2004; Dunbar & Kurbatov, 2011;  
73 Abram et al., 2011; Mulvaney et al., 2012; Koffman et al., 2013; Goodwin, 2013; Thomas &  
74 Abram, 2016). Most studies have focused on detecting large explosive tropical eruptions  
75 (Pinatubo (1991), Agung (1963), Tambora (1815), among others) to establish absolute time  
76 markers for ice core chronologies or set tie-points to synchronize different records. Only a few  
77 studies document regional volcanism, mostly focused on volcanic activity in Deception Island,  
78 off the northern Antarctic Peninsula (Aristarain & Delmas, 1998; Jiankang et al., 1999; Dunbar  
79 et al., 2003; Mulvaney et al., 2012; Koffman et al., 2013).

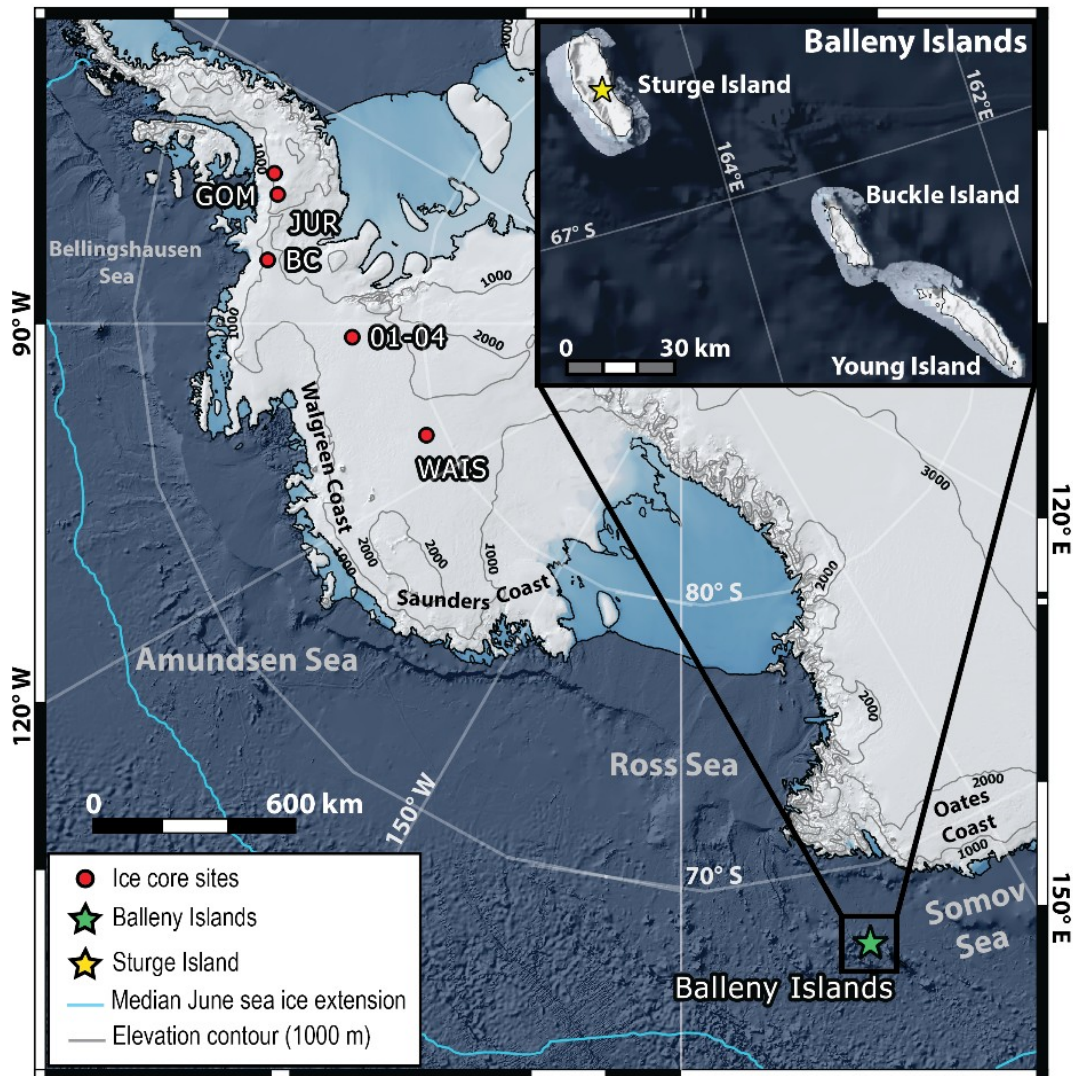
80 The Balleny Islands are a chain of volcanic islands off the coast of Victoria Land,  
81 Antarctica. Sturge Island (1167 m a.s.l) is the largest and southernmost island in the volcanic  
82 chain (LeMasurier et al., 1990). This island is a stratovolcano covered by an icecap with no  
83 records of present or past volcanic activity (Hund, 2014). On 12<sup>th</sup> of June 2001 (1352 UTC), an  
84 unusual cloud formation was spotted over Sturge Island by the U.S. National Ice Center using  
85 Optical Line Scan Imagery and was still visible, attached to the island, on MODIS imagery at  
86 2245 UTC. Satellite imagery analyses determined the cloud was a single feature in the region,  
87 reaching a visible extension of 300 km downwind (E-NE), with a maximum cloud top at  
88 approximately 6 km and revealed the possible presence of volcanic SO<sub>2</sub>. However, the same  
89 analyses revealed the absence of ash in the cloud, presenting the satellite imagery data alone as  
90 inconclusive to determine if the cloud was produced by a volcanic eruption in Sturge Island  
91 (Global Volcanism Program, 2001).

92 Here we present a detailed study of five ice core glaciochemical and microparticle  
93 records from the southern Antarctic Peninsula, Ellsworth Land and Marie Byrd Land, to validate  
94 the occurrence of recent active volcanism in the Balleny Islands. Forward air mass trajectories  
95 are used to track the air masses originating from the Balleny Islands at the time of the potential  
96 2001 eruption. Additionally, we include the analysis of insoluble particle matter in the ice cores  
97 and explore the presence of cryptotephra as absolute markers of volcanic activity. The aim of this  
98 study is to provide independent ice core evidence for a 2001 volcanic eruption on Sturge Island  
99 and present a potential absolute age-marker for Antarctic ice core chronologies.

## 100 **2 Methods**

### 101 2.1 Study sites

102 Five ice cores from the southern Antarctic Peninsula, Ellsworth Land and Marie Byrd  
103 Land were included in this study (Figure 1) (Table 1). The cores were selected due to their  
104 downwind location from the Balleny Islands, their retrieval after the 2001 austral winter, their  
105 temporal resolution (>10 samples in the youngest year), their regional distribution and their data  
106 availability. Among the five ice cores used in this study, four (GOM, BC, 01-4, WAIS) have  
107 been previously published (Table 1). The 140 m Jurassic ice core (JUR) was drilled by the  
108 British Antarctic Survey on the English Coast, Southern Antarctic Peninsula during the austral  
109 summer 2012/2013. Ice core samples were cut using a band-saw with a steel blade and then  
110 melted using a Continuous Flow Analysis (CFA) system (Rothlisberger et al., 2000) in the ice  
111 chemistry lab at the British Antarctic Survey, UK. An ice core chronology was established based  
112 on the hydrogen peroxide annual cycle that is assumed to peak during the summer solstice. The  
113 top 53.5 m included in this work were dated back to 1977 AD, with an estimated dating error for  
114 the 1977-2013 interval of  $\pm 3$  months for each year and with no accumulated error. Discrete ice  
115 core samples were cut at 5 cm resolution for major ion analysis (including Methanesulphonic  
116 Acid (MSA), sodium and sulphate) with ion chromatography, using a reagent-free Dionex ICS-  
117 2500 anion and IC 2000 cation system.



118

119 **Figure 1.** Map showing the ice core sites considered in this study. The red circles show the  
 120 locations of the five ice core sites. The yellow star shows the location of Sturge Island in the  
 121 Balleny Islands (green star). The light blue line shows the median June sea ice-extension  
 122 between 1980-2010 AD

123 Four ice cores (GOM, JUR, BC and WAIS) were evaluated over a 30-year overlapping  
 124 period (1977-2007 AD) for evidence of a volcanic eruption in the 2001 ice layer (hereafter  
 125 referred to as 2001L). The ITASE 01-4 ice core, drilled in 2002, was evaluated over a 25-year  
 126 overlapping period (1977-2002 AD). Additionally, two previously identified ice core horizons  
 127 were targeted as examples of well-dated recent volcanic events recorded in ice core layers. The  
 128 1994-1992 AD horizon for the Mount Pinatubo and Cerro Hudson eruption (Pinatubo/Hudson)  
 129 (1991 AD) (Cole-Dai & Mosley-Thompson, 1999; Zhang et al., 2002; Jiang et al., 2012;  
 130 Plummer et al., 2012; Osipov et al., 2014; Schwanck et al., 2017; Thoen et al., 2018; Hoffmann  
 131 et al., 2020) and the 1984-1982 AD horizon for the El Chichón eruption (1982 AD) (Traufetter et  
 132 al., 2004; Jiang et al., 2012; Plummer et al., 2012; Thoen et al., 2018). Both eruptions are  
 133 observed in younger ice core horizons because of the lagged deposition of volcanic sulphates

134 over the Antarctic ice sheet after large low-latitude eruptions (Cole-Dai et al., 1997). All ages  
135 presented in this work are based on the ice chronologies reported for each core (Table1).

136 **Table 1.** Summary of each ice core geographical location and main features of the datasets  
137 analysed in this study. Abbr: Abbreviation.

138

Core Name	Abbr.	Long	Lat	Elevation (m a.s.l.)	Year drilled (AD)	Depth interval (m)	Sample resolution (m)	Ice chronology
Gomez	GOM	-70.36	-73.59	1400	2007	0-45.48	0.02	Thomas et al., 2008
Jurassic Bryan Coast	JUR BC	-73.06 -81.67	-74.33 -74.49	1139 1177	2013 2011	10.14-53.5 4.41-28.45	0.05 0.05	This work Thomas et al., 2015
ITASE 01-4	01-4	-92.25	-77.61	1483	2002	0-16.56	0.03	Mayewski & Dixon, 2005
WAIS Divide	WAIS	-112.09	-79.47	1797	2007	0-12.50	0.03	Sigl et al. 2016

## 139 2.2 Sulphate concentration analyses

140 Sulphate from volcanic eruptions is superimposed over the background sulphate. This  
141 includes organic sulphur compounds, such as dimethyl sulphide (DMS), from marine biogenic  
142 emissions (Maupetit & Delmas, 1992; Cole-Dai et al., 2000; Castellano et al., 2004; Dixon et al.,  
143 2004; Nardin et al., 2020), with a smaller contribution from sea salt aerosols. Even though the  
144 background sulphate is temporally variable, it can be assumed as relatively constant in the last  
145 centuries (Kreutz et al., 1999; Kreutz et al., 2000; Traversi et al., 2002; Castellano et al., 2004).  
146 Therefore, for the detection of volcanic signals, it is crucial that the correct assessment of the  
147 background sulphate concentration, and its variability is established. In particular, the accurate  
148 detection of small and moderate volcanic events depends on how the background sulphate is  
149 quantified and the volcanic detection threshold established (Cole-Dai et al., 1997; Budner &  
150 Cole-Dai, 2003; Castellano et al., 2004). Several methods have been proposed (Cole-Dai et al.,  
151 1997; Castellano et al., 2004; Traufetter et al., 2004; Gautier et al 2016) based on the evaluation  
152 of a background sulphate representative value ( $m$ ) and its standard deviation ( $\sigma$ ) to establish a  
153 threshold ( $m+2\sigma$ ). Sulphate peaks above this threshold are considered indicative of volcanic  
154 activity.

155 In this work, the background signal is evaluated in the total sulphate concentration  
156 ( $\text{SO}_4^{2-}$ ) and in the non-sea salt sulphate flux ( $\text{nssSO}_4^{2-}$ -flux) (Cole-Dai et al., 1997). The  $\text{nssSO}_4^{2-}$ -  
157 flux was calculated using Equation 1 and Equation 2 (Wagenbach et al., 1998), and using sodium  
158 ( $\text{Na}^+$ ) as the reference ion (Castellano et al., 2004; Dixon et al., 2004; Ren et al., 2010; Li et al.,  
159 2012; Jiang et al., 2012; Osipov et al., 2014). The analysis of the  $\text{nssSO}_4^{2-}$ -flux was incorporated  
160 because it facilitates the detection of small and moderate volcanic signals (Cole-Dai et al., 1997;  
161 Zhang et al., 2002). In the absence of sulphate data from the GOM ice core, the total sulphur  
162 ( $S_{\text{tot}}$ ) and non-sea salt sulphur flux ( $\text{nssS}$ -flux) were used for calculations.

163 
$$i = \frac{S_{\text{tot}} - \text{nssS}}{S_{\text{tot}}} \quad (\text{Equation 1})$$

164 
$$\text{nssS} = O_4^{2-} \text{flux} - i \text{flux} \quad (\text{Equation 2})$$

165 To detect volcanic eruptions from elevated  $\text{SO}_4^{2-}$  and  $\text{nssSO}_4^{2-}$ -flux, we applied the  
166 method originally proposed by Castellano et al. (2004). This method was selected over other  
167 methods (Cole-Dai et al., 1997; Traufetter et al., 2004) because it considers the lognormal  
168 distribution of the sulphate data. The use of lognormal statistics in sulphate analyses has been  
169 proven to clearly differentiate between volcanic sulphate and background sulphate (Castellano et  
170 al., 2004). To calculate the background sulphate, new datasets were generated after excluding  
171 individual ice core horizons from well-known volcanic eruptions between 2007-1977 AD (e.g.  
172 Pinatubo/Hudson (1991 AD) and El Chichón (1982 AD)). After excluding these horizons, the  
173 background and its variability were estimated at each sample point by calculating in the log  
174 domain, the mean and standard deviation of a 20% weighted curve fit centred on each sample  
175 point (10% weighted curve fit for the shorter 01-4 ice core). To identify samples with a potential  
176 volcanic influence, the  $\text{SO}_4^{2-}$  and  $\text{nssSO}_4^{2-}$ -flux had to exceed the background signal (m) by two  
177 times the standard deviation ( $>2\sigma$ -peak). This threshold ensured 95.5% of the random  
178 background variability was excluded.  $\text{SO}_4^{2-}$  and  $\text{nssSO}_4^{2-}$ -flux  $>2\sigma$ -peaks were classified based on  
179 the number of data points exceeding the threshold (single point (=1) or multiple points ( $>1$ )). The  
180 method applied in this study assumes that in the absence of inputs from large volcanic and  
181 anthropogenic sources (negligible in Antarctica), the sulphate concentration in the snow  
182 comprises inputs from regional background sulphate emissions, not controlled by a dominant  
183 source region or transport and deposition processes (Cole-Dai et al., 1997).  $S_{\text{tot}}$  and  $\text{nssS}$ -flux  
184 from GOM were analysed using the same method applied for  $\text{SO}_4^{2-}$  and  $\text{nssSO}_4^{2-}$ -flux volcanic  
185 detection analyses, respectively.

186 As previously stated, one of the main sources of background sulphate is DMS from  
187 marine biogenic emissions. The oxidation of DMS in the atmosphere produces MSA, a chemical  
188 compound widely studied in ice core records because of its link to marine biogenic emissions in  
189 the Southern Ocean (Curran et al., 2003; Abram et al., 2010; Abram et al., 2013; Criscitiello et  
190 al., 2013; Thomas et al., 2016). The MSA records available for GOM, JUR and BC ice cores are  
191 included to assess whether the  $\text{SO}_4^{2-}$   $>2\sigma$ -peaks identified in the 2001L were influenced by  
192 increased marine biogenic emissions. MSA records for WAIS and 01-4 ice cores were not  
193 available.

194 The total  $\text{Na}^+$  concentration in ice is largely determined by the interaction of airmasses  
195 with marine open waters and potential short-term inputs from volcanic ash (Legrand &  
196 Mayewski, 1997). Since the  $\text{nssSO}_4^{2-}$ -flux is calculated using  $\text{Na}^+$  as the reference ion, it is  
197 crucial to study the variability of  $\text{SO}_4^{2-}$  and  $\text{Na}^+$ . The  $\text{Na}^+$  record from each of the five ice cores  
198 was included to assess whether the  $\text{nssSO}_4^{2-}$ -flux values in the 2001L were influenced by  
199 additional inputs from non-volcanic sources.

200 Volcanic sulphate fluxes were calculated for two of the targeted periods (2001L and  
201 1992-1994 AD). The 1984-1982 AD horizon for the El Chichón eruption (1982 AD) was not  
202 included due to the lack of  $>2\sigma$ -peaks in the  $\text{nssSO}_4^{2-}$ -flux profiles. To calculate the volcanic  
203 sulphate flux, the background  $\text{nssSO}_4^{2-}$ -flux was subtracted from the sample  $\text{nssSO}_4^{2-}$ -flux on  
204 each volcanic event identified ( $>2\sigma$ -peak). Therefore, the total flux for a volcanic event is the  
205 sum of all the residuals of  $\text{nssSO}_4^{2-}$ -flux samples from the corresponding layers and over the  
206 background  $\text{nssSO}_4^{2-}$ -flux (Jiang et al., 2012). Where elevated  $\text{nssSO}_4^{2-}$ -flux does not exceed the  
207 detection threshold ( $m+2\sigma$ ), the volcanic sulphate flux was calculated as the sum of  $\text{nssSO}_4^{2-}$ -flux  
208 residuals within the depth interval where a  $\text{SO}_4^{2-}$   $>2\sigma$ -peak was identified. To compare the 2001L  
209 volcanic sulphate fluxes among different ice cores, the 2001L  $\text{nssSO}_4^{2-}$ -flux was normalized

210 against the  $\text{nssSO}_4^{2-}$ -flux of the well-documented Pinatubo/Hudson eruption (Cole-Dai, et al.,  
211 1997). Due to the different parameters measured in GOM ( $S_{\text{tot}}$  and  $\text{nssS}$ -flux), this ice core was  
212 excluded from the volcanic sulphate flux calculations.

### 213 2.3 Physical properties analyses

214 The electrical conductivity (EC) signal recorded in ice is controlled by soluble impurities  
215 that originate mostly from sea salt, biomass burning, and volcanic eruptions, and is strongly  
216 correlated with acidity (Mulvaney, 2013). EC measurements from four ice cores were included  
217 in this study (only available at GOM, JUR, BC and WAIS) as an additional dataset to test the  
218 presence of volcanic products. EC was analysed in different labs using an Amber Science flow-  
219 through meter connected to a continuous ice core melter system. EC data presented a log-normal  
220 distribution. Therefore, data treatment and calculations were performed using log-normal  
221 statistics. The background conductivity, its variability and the establishment of an anomalous  
222 conductivity detection threshold were calculated following the same method presented in section  
223 2.2 for  $\text{SO}_4^{2-}$  and  $\text{nssSO}_4^{2-}$ -flux.

### 224 2.4 Forward trajectory analyses

225 Forward trajectory analysis is used to examine the pathways of air masses passing over  
226 the Balleny Islands and their potential transit over the ice core sites during the deposition of the  
227 2001L. The National Oceanic and Atmospheric Administration (NOAA)'s Hybrid Single-  
228 Particle Lagrangian Integrated Trajectory (HYSPPLIT) model (Draxler & Hess, 1998; Stein et al.,  
229 2015) was used to calculate three-dimensional air parcel pathways under isobaric conditions (2.5  
230 degree latitude-longitude resolution). Trajectories were calculated starting from the Balleny  
231 Islands for a 30-hour interval, 15 hours before and 15 hours after the first evidence of possible  
232 volcanic activity (1352 UTC on 12 June 2001). Forward trajectories were initiated every hour for  
233 up to 10 days using the NCEP/NCAR Reanalysis archives (1948 - present) with three starting  
234 elevations: 1000, 1500 and 2000 meters above the sea level (a.s.l.). These elevations were  
235 selected because of their close proximity to the summit of Sturge Island (1167 m a.s.l.), from  
236 where a potential volcanic plume could have been emitted. For comparison, trajectories were  
237 classified into three groups based on their starting time relative to the first remote sensing (RS)  
238 evidence of the unusual cloud formation over Sturge Island: pre-RS evidence, first-RS evidence  
239 and post-RS evidence.

### 240 2.5 Microparticle analyses

241 Microparticle Concentration (MPC) and Particle Size Distributions (PSD) were  
242 measured. Microparticle data was obtained from the JUR and WAIS ice cores. The later  
243 corresponds to the WAIS Divide deep ice core, WDC06A (Kreutz et al., 2011; Kreutz et al.,  
244 2015). MPC from the WDC06A was measured using a flow-through Klotz Abakus laser particle  
245 counter connected to a continuous ice core melter system at the University of Maine (Breton et  
246 al., 2012). Particles were measured in 31 size channels, spanning 115  $\mu\text{m}$  diameter. Similarly,  
247 MPC from the JUR ice core was measured using a flow-through Klotz Abakus laser particle  
248 counter connected to a continuous ice core melter system at the British Antarctic Survey.  
249 Particles were measured in 23 size channels spanning 0.9-12  $\mu\text{m}$  diameter. MPC datasets  
250 presented a log-normal distribution. Therefore, data treatment and calculations were performed  
251 using log-normal statistics. To assess whether a MPC peak in the dataset could be influenced by  
252 volcanic activity, the microparticle background concentration and its variability were calculated.

253 A detection threshold was set following the same guidelines presented in section 2.2 for sulphate  
254 analyses. The JUR dust record is presented with a 4-meter gap, due to problems in the data  
255 acquisition between 43.6-47.6 meters deep.

256 PSD were obtained by calculating the ratio of total volume of insoluble dust contained  
257 within each size bin and the derivative of the volume with respect to the natural logarithm of the  
258 particle diameter for each bin ( $dV/d\ln D$ ), as presented in Koffman et al. (2014). Three individual  
259 ice core horizons were targeted to characterize their PSD: The 2001 ice core horizon (2001L),  
260 Pinatubo/Hudson eruption (1991 AD) and El Chichón eruption (1982 AD). To determine if the  
261 targeted horizons differ from the background particle size of atmospheric dust, the PSD for the  
262 1977-2007 AD period was calculated as the average PSD after removing the three targeted  
263 horizons. For PSD analyses, the mode particle diameter as a representative statistic of the volume  
264 distribution was used (Ruth et al., 2003; Koffman et al., 2014).

265 Microscopy analyses of microparticles were included to determine whether any of the  
266 particles present in the 2001 AD horizon were cryptotephra shards. For this, ice samples of 200  
267 mL, from the 2001L of the JUR and GOM ice cores, were melted and filtered. Samples were  
268 melted using a Continuous Flow Analysis (CFA) system (Rothlisberger et al., 2000) in the ice  
269 chemistry lab at the British Antarctic Survey, UK. Meltwater from the CFA waste lines was  
270 collected in new bottles then filtered through 13 mm diameter, 1.0  $\mu\text{m}$  pore size Whatman™  
271 Polycarbonate membrane filters, inside clean polypropylene Swinnex™ filter holders. Filters  
272 were mounted onto aluminium stubs for analyses on a Scanning Electron Microscope (SEM) at  
273 the Earth Sciences Department of the University of Cambridge. Filters were imaged on a  
274 Quanta-650F using Back Scattered Electrons (BSE) on a low-pressure mode. Each filter was  
275 imaged at x800 magnification for cryptotephra identification and physical characterization,  
276 following the analysis strategy presented in Tetzner et al. (2021). Two additional samples from  
277 the 2001L of the JUR ice core were melted in a class-100 clean room, then centrifuged (6 mins at  
278 1200/1600 rpm) and decanted successively until samples were concentrated in 2–5 mL fluid. The  
279 2–5 mL sample liquid was homogenised, pipetted onto a single coverslip (22 × 40 mm), dried in  
280 an isolated drying cupboard and then mounted onto a single microscope slide using Norland  
281 optical adhesive 61 (refractive index 1.56). Each microscope slide was scanned for the presence  
282 of cryptotephra shards.

## 283 **3 Results**

### 284 3.1 Geochemical analyses

#### 285 3.1.1 Sulphate concentration profiles

286 For each core, numerous  $\text{SO}_4^{2-}$  peaks were identified (GOM (9), JUR (7), BC (6), WAIS  
287 (3) and 01-4 (14)) as exceeding the volcanic detection threshold ( $m+2\sigma$ ) (Figure 2). The most  
288 prominent were almost exclusively associated with the target intervals with volcanic activity  
289 (2001, 1994-1992 and 1984-1982). Table 2 presents the main features for each of those peaks.

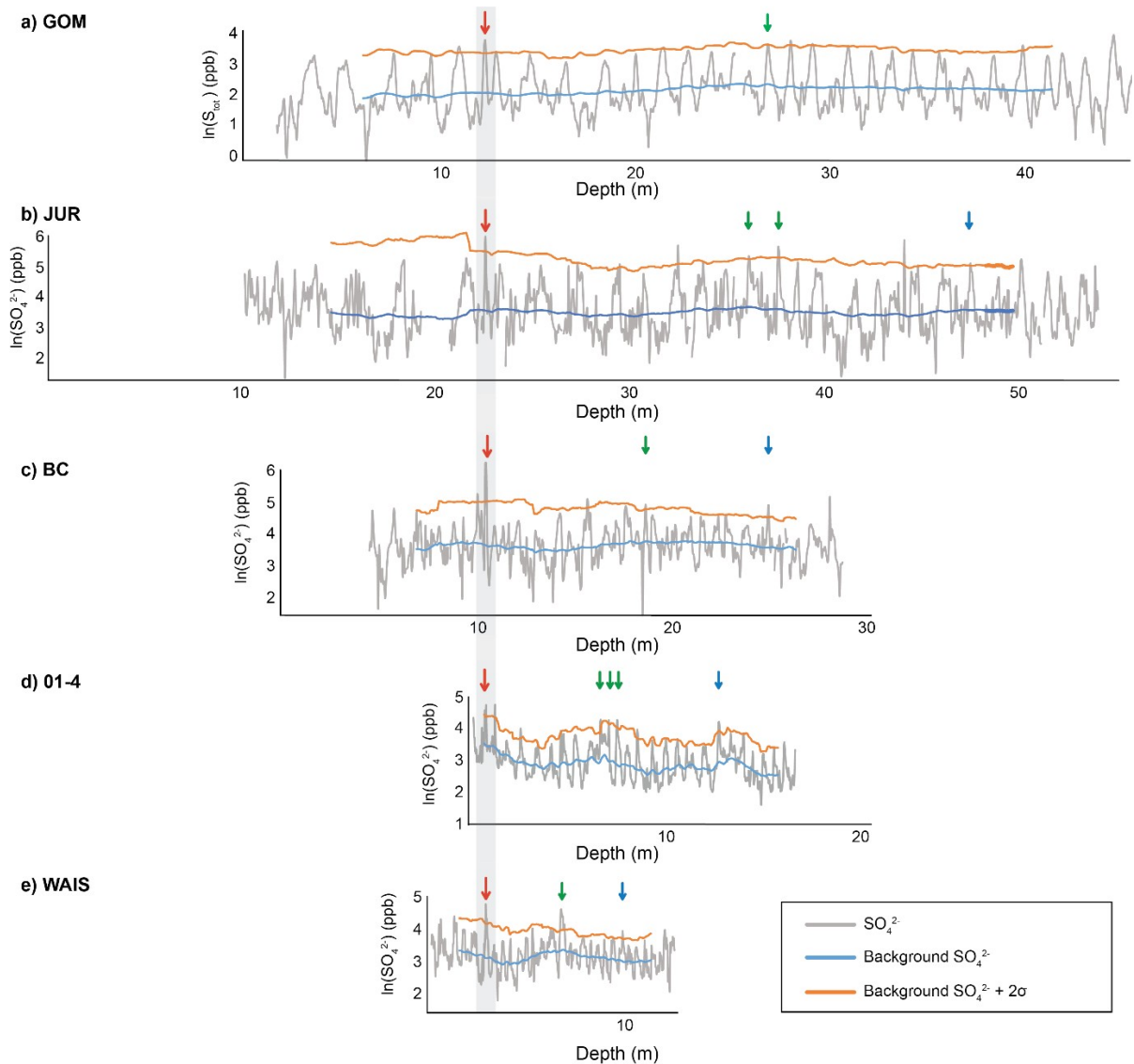
290 The 2001L present the most prominent  $\text{SO}_4^{2-}>2\sigma$ -peaks during the 1977-2007 AD period,  
291 all of them presenting an order of magnitude increase above the background.  $\text{SO}_4^{2-}>2\sigma$ -peaks in  
292 the 2001L are characterized either by a sharp peak during mid-2001 (GOM, JUR, BC and 01-4)  
293 or by a wide 2001/2000 austral summer peak (WAIS). The  $\text{SO}_4^{2-}>2\sigma$ -peaks identified within the  
294 1994-1992 AD ice core layer are characterized by single (GOM, BC and WAIS) or multiyear

295 sulphate increases (JUR and 01-4) during the austral summer 1991/1992 AD or 1992/1993 AD.  
 296  $\text{SO}_4^{2-}$ > $2\sigma$ -peaks identified within the 1984-1982 AD ice core layer are consistently smaller than  
 297 the peaks identified in the other targeted periods and are characterized by a single increase in the  
 298  $\text{SO}_4^{2-}$  concentration during the austral summer 1983/1984 AD.

299 **Table 2.** Summary of the main features of  $\text{SO}_4^{2-}$  and  $\text{nssSO}_4^{2-}$ -flux> $2\sigma$ -peaks above the volcanic  
 300 detection threshold within the targeted periods (2001, 1992-1994, 1982-1984 AD).

301

Core	Depth interval of excess sulphate (m)	Year in ice chronology (AD)	Data points above the threshold
<b><math>\text{SO}_4^{2-}</math></b>			
GOM	12.16 - 12.44	2001	>1
	26.52 - 26.98	1991/1992	>1
JUR	22.30 - 22.41	2001	1
	35.64 - 36.34	1992/1993	>1
	37.19 - 37.49	1991/1992	>1
	46.90 - 47.20	1982/1983	1
BC	10.25 - 10.4	2001	>1
	18.34 - 18.54	1992/1993	1
	24.54 - 24.74	1982/1983	>1
01-4	0.56 - 0.7	2001	>1
	6.46 - 6.99	1992/1993	>1
	7.34 - 7.59	1991/1992	>1
	12.55 - 12.73	1983/1984	>1
WAIS	2.72 - 2.93	2000/2001	>1
	6.60 - 6.93	1992/1993	>1
	9.66 - 9.97	1983	1
<b><math>\text{nssSO}_4^{2-}</math>-flux</b>			
GOM	26.52 - 26.98	1991/1992	>1
JUR	37.19 - 37.49	1991/1992	1
01-4	0.56 - 0.7	2001	>1
	6.46 - 6.99	1992/1993	>1
WAIS	12.55 - 12.73	1983/1984	>1
	2.72 - 2.93	2000/2001	1
	6.60 - 6.93	1992/1993	>1



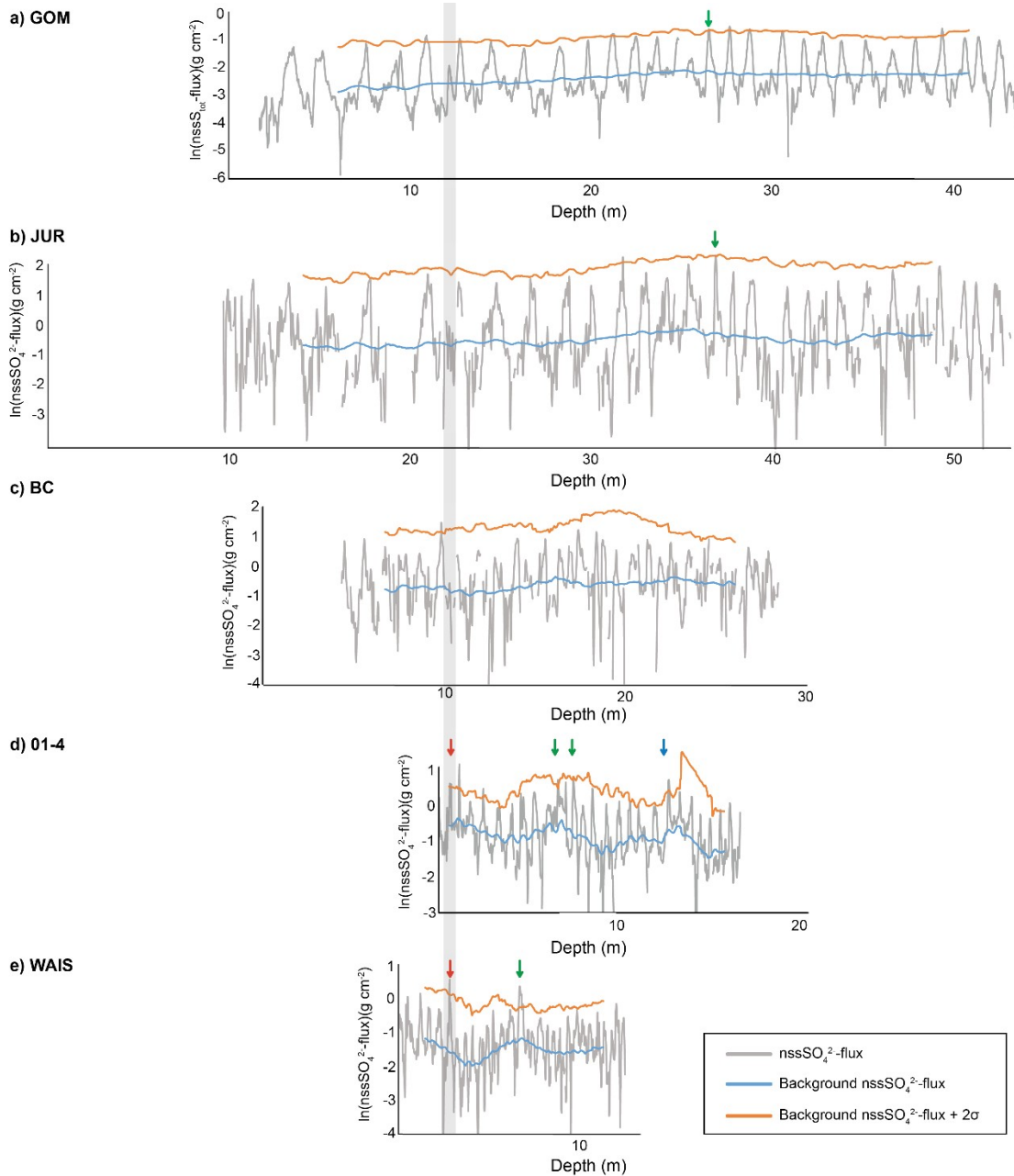
302

303 **Figure 2.**  $\text{SO}_4^{2-}$  profiles of the depth intervals corresponding to the 1977-2007 AD period for the  
 304 five ice cores considered in this study. Arrows identify  $\text{SO}_4^{2-}$  peaks above the detection threshold  
 305 ( $m+2\sigma$ ). Red arrows indicate peaks above the detection threshold in the 2001 AD ice core layer.  
 306 Green arrows indicate peaks above the detection threshold in the 1994-1992 AD ice core layer.  
 307 Blue arrows indicate peaks above the detection threshold in the 1984-1982 AD ice core layer.  
 308 The grey band highlights the 2001 AD ice core layer.

### 309 3.1.2 nss $\text{SO}_4^{2-}$ -flux profiles

310 Twenty peaks were identified exceeding the nss $\text{SO}_4^{2-}$ -flux volcanic detection threshold  
 311 (nss $\text{SO}_4^{2-}$ -flux  $> 2\sigma$ ): GOM (8); JUR (2); BC (1); WAIS (2) and 01-4 (7) (Figure 3). All had been  
 312 previously identified as  $\text{SO}_4^{2-} > 2\sigma$ -peaks (Figure 2). Among the nss $\text{SO}_4^{2-}$ -flux  $> 2\sigma$ -peaks detected,  
 313 eight occurred within the targeted periods. Table 2 presents the main features for each of these  
 314 eight peaks.

315 The most consistent and prominent  $\text{nssSO}_4^{2-}$ -flux $>2\sigma$ -peaks were identified in the 1993-  
 316 1992 AD ice core layers. The 2001L exhibited  $\text{nssSO}_4^{2-}$ -flux $>2\sigma$ -peaks in WAIS and 01-4. The  
 317 1982-1984 AD period was represented only by a single  $\text{nssSO}_4^{2-}$ -flux $>2\sigma$ -peak in the 01-4 core  
 318 during the austral summer 1983/1984 AD.



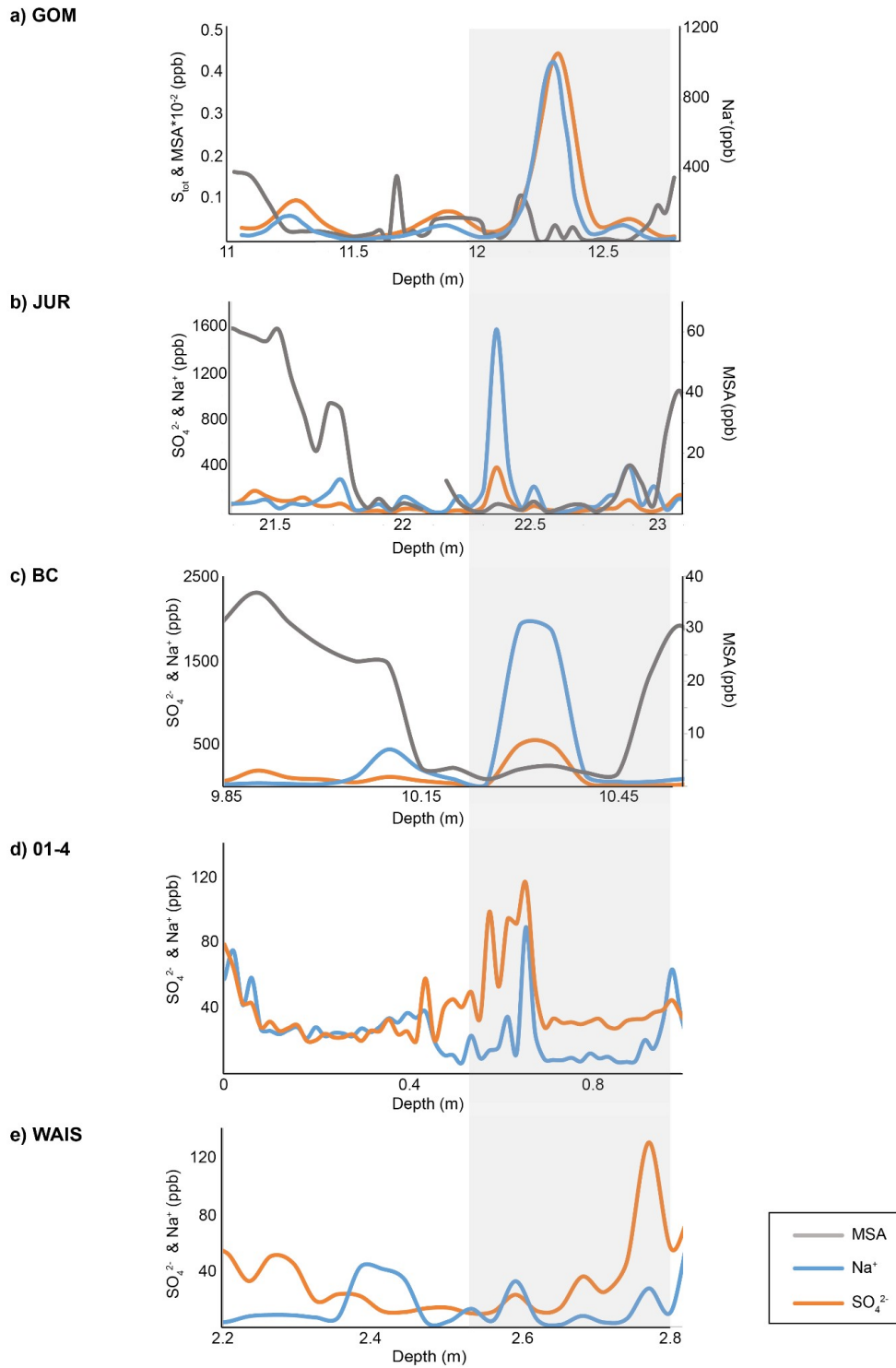
319

320 **Figure 3.**  $\text{nssSO}_4^{2-}$ -flux profiles of the depth interval corresponding to the 1977-2007 AD period  
 321 for the five ice cores considered in this study. Arrows identify peaks above the detection  
 322 threshold. Red arrows indicate peaks above the detection threshold in the 2001 AD ice core  
 323 layer. Green arrows indicate peaks above the detection threshold in the 1994-1992 AD ice core  
 324 layer. Blue arrows indicate peaks above the detection threshold in the 1984-1982 AD ice core  
 325 layer. The grey band highlights the 2001 AD ice core layer.

326 3.1.2 Methanesulphonic Acid (MSA) and sodium measurements

327 MSA profiles for JUR and BC from 2001L presented prominent peaks of >35 ppb  
328 indicative of spring/summer periods and a minimum <5 ppb, denoting the autumn/winter interval  
329 (Figure 4). The GOM MSA profile exhibit peaks of >15 ppb indicative of spring/summer and  
330 slightly smaller, isolated MSA events that correlate with autumn/winter timing e.g. at 11.71 and  
331 12.20 meters deep.

332 Prominent Na<sup>+</sup> peaks of >1000 ppb were identified at 12.3, 10.35, and 22.36 meters deep  
333 in GOM, JUR and BC, respectively (Figure 4). These peaks were more than an order of  
334 magnitude above the background Na<sup>+</sup>. Smaller increases of ~30 (ppb) in Na<sup>+</sup> were identified in  
335 01-4 and WAIS. The 01-4 ice core presented a distinct 6-fold increase (53.15 ppb) in Na<sup>+</sup> over  
336 the background at 0.66 meters deep. WAIS presented a minor increase of ~20 ppb in Na<sup>+</sup> at 2.80  
337 meters deep.



338

339 **Figure 4.** MSA, SO<sub>4</sub><sup>2-</sup> and Na<sup>+</sup> profiles for depth interval corresponding to the 2001 AD ice core  
 340 layer (2001L). The grey band highlights the January-July period in the 2001 AD ice core layer.

341

## 342 3.1.4 Volcanic sulphate flux

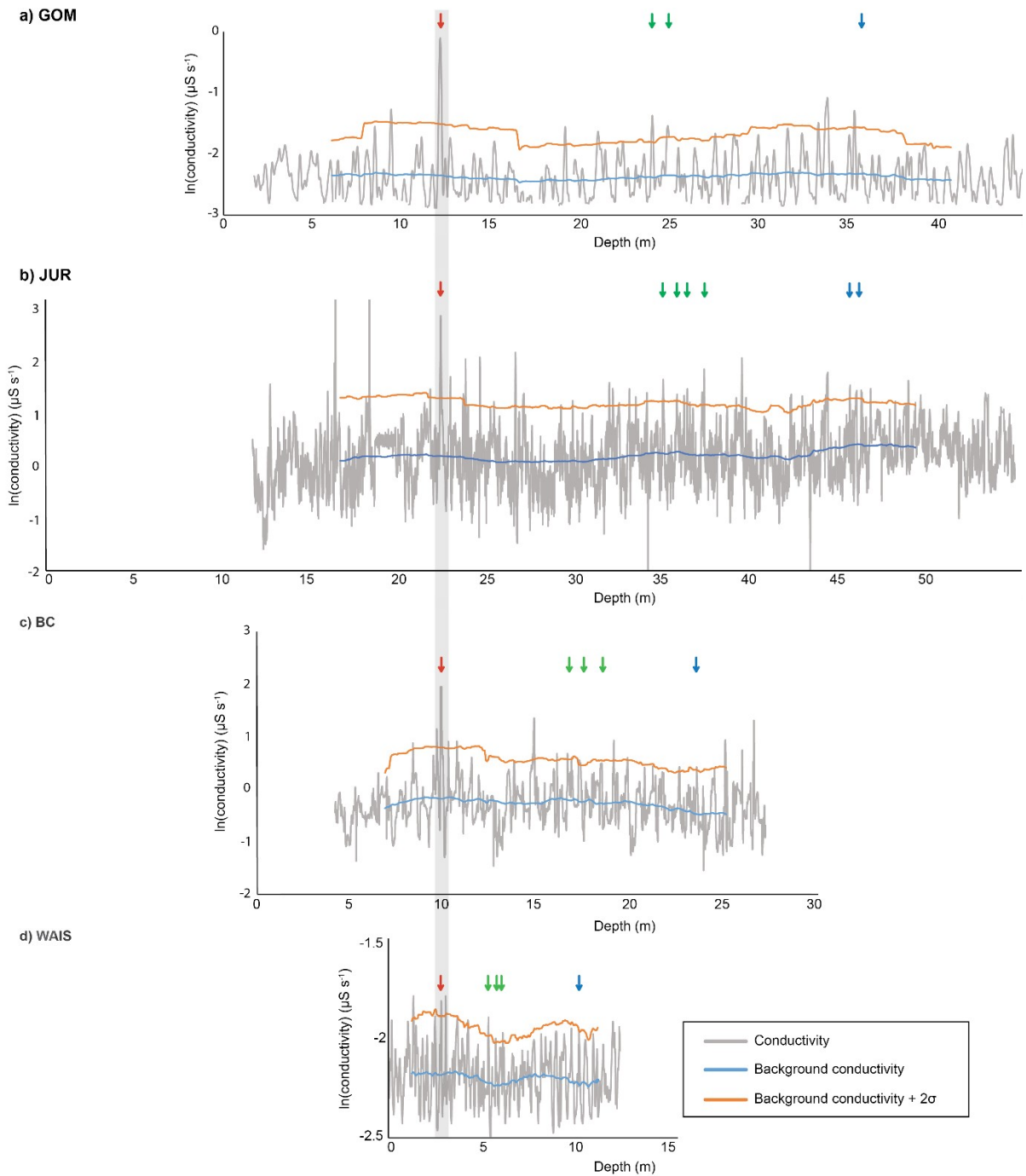
343 The net volcanic sulphate fluxes (VSF) for 2001L and 1993-1992 AD were calculated  
 344 (Table 3). The VSF ratio (2001L:1993-1992) exhibited a spatial gradient with higher values  
 345 ( $>0.42$ ) for ice cores from Ellsworth Land-Marie Byrd Land (WAIS, O1-4) and considerably  
 346 lower values ( $<0.03$ ) for ice cores from the southern Antarctic Peninsula (BC, JUR & GOM).

347 **Table 3.** Volcanic sulphate fluxes for the 2001 and 1993-1992 ice core layers.

Core	VSF (2001L)(g cm <sup>-3</sup> )	VSF (1993-1992 AD) (g cm <sup>-3</sup> )	VSF ratio
Jurassic	0.62	22.77	0.03
Bryan Coast	0.14	5.12	0.03
O1-4	1.98	4.64	0.43
WAIS	3.77	8.13	0.46

## 348 3.2 Electrical conductivity (EC) profiles

349 EC profiles from four ice cores (GOM, JUR, BC and WAIS) were examined during the  
 350 1977-2007 AD period (Figure 5). In the GOM EC profile, eleven peaks were identified  
 351 exceeding the conductivity threshold ( $EC > 2\sigma$ -peak). The most prominent identified at 12.24 m  
 352 ( $0.898 \mu\text{S s}^{-1}$ ), 24.22 m ( $0.249 \mu\text{S s}^{-1}$ ) and 34.12 m ( $0.335 \mu\text{S s}^{-1}$ ), corresponding to years 2001,  
 353 1993 and 1986 AD. In the JUR EC profile, twenty-four  $EC > 2\sigma$ -peaks were identified, with the  
 354 most prominent found at 18.32 m ( $3.21 \mu\text{S s}^{-1}$ ) and 22.38 m ( $1.5 \mu\text{S s}^{-1}$ ), corresponding to 2003  
 355 and 2001 AD. In the BC EC profile, fourteen  $EC > 2\sigma$ -peaks were identified, the most prominent  
 356 at 10.28 m ( $0.701 \mu\text{S s}^{-1}$ ), 15.52 m ( $0.385 \mu\text{S s}^{-1}$ ) and 26.2 m ( $0.254 \mu\text{S s}^{-1}$ ) corresponding to  
 357 2001, 1996 and 1982 AD. In the WAIS EC profile, eight  $EC > 2\sigma$ -peaks were identified, the most  
 358 prominent occurring at 1.33 m ( $0.167 \mu\text{S s}^{-1}$ ), 2.82 m ( $0.163 \mu\text{S s}^{-1}$ ), 3.07 m ( $0.167 \mu\text{S s}^{-1}$ ) and  
 359 5.36 m ( $0.150 \mu\text{S s}^{-1}$ ), corresponding to years 2003, 2001, 2000 and 1994 AD. Three of the  
 360  $EC > 2\sigma$ -peaks were common to all four sites corresponding to years 2003, 2001 and 1994-1993.  
 361 The 2001 peak was among the most prominent  $EC > 2\sigma$ -peaks in each EC profile (Figure 5).



362

363 **Figure 5.** EC profiles for GOM, JUR, BC and WAIS for the depth interval corresponding to the  
 364 1977-2007 AD period. Red arrows indicate peaks above the detection threshold ( $m+2\sigma$ ) in the  
 365 2001 AD ice core layer. Green arrows indicate peaks above the detection threshold in the 1994-  
 366 1992 AD ice core layer. Blue arrows indicate peaks above the detection threshold in the 1984-  
 367 1982 AD ice core layer. The grey band highlights the 2001 AD ice core layer.

### 368 3.3 Microparticle analyses

#### 369 3.3.1 Microparticle concentration (MPC)

370 The MPC (particles per mL – p mL<sup>-1</sup>) was examined during the 1977-2007 AD period  
371 (Figure 6a and Figure 6b). In WAIS, ten peaks exceeded the MPC threshold. The most  
372 prominent corresponding to the 1991-1992 AD period (6.78-6.96 m, 4257 p mL<sup>-1</sup>) and smaller  
373 peaks corresponding to 1982 and 2001-2000 AD (2.84 m, 2915 p mL<sup>-1</sup>). In JUR, nine peaks were  
374 identified. The most prominent corresponding to 1991-1992 AD (37.38 m, 6510 p mL<sup>-1</sup>) with  
375 smaller peaks identified corresponding to 1982 and 2001 AD.

#### 376 3.3.2 Particle size distribution (PSD)

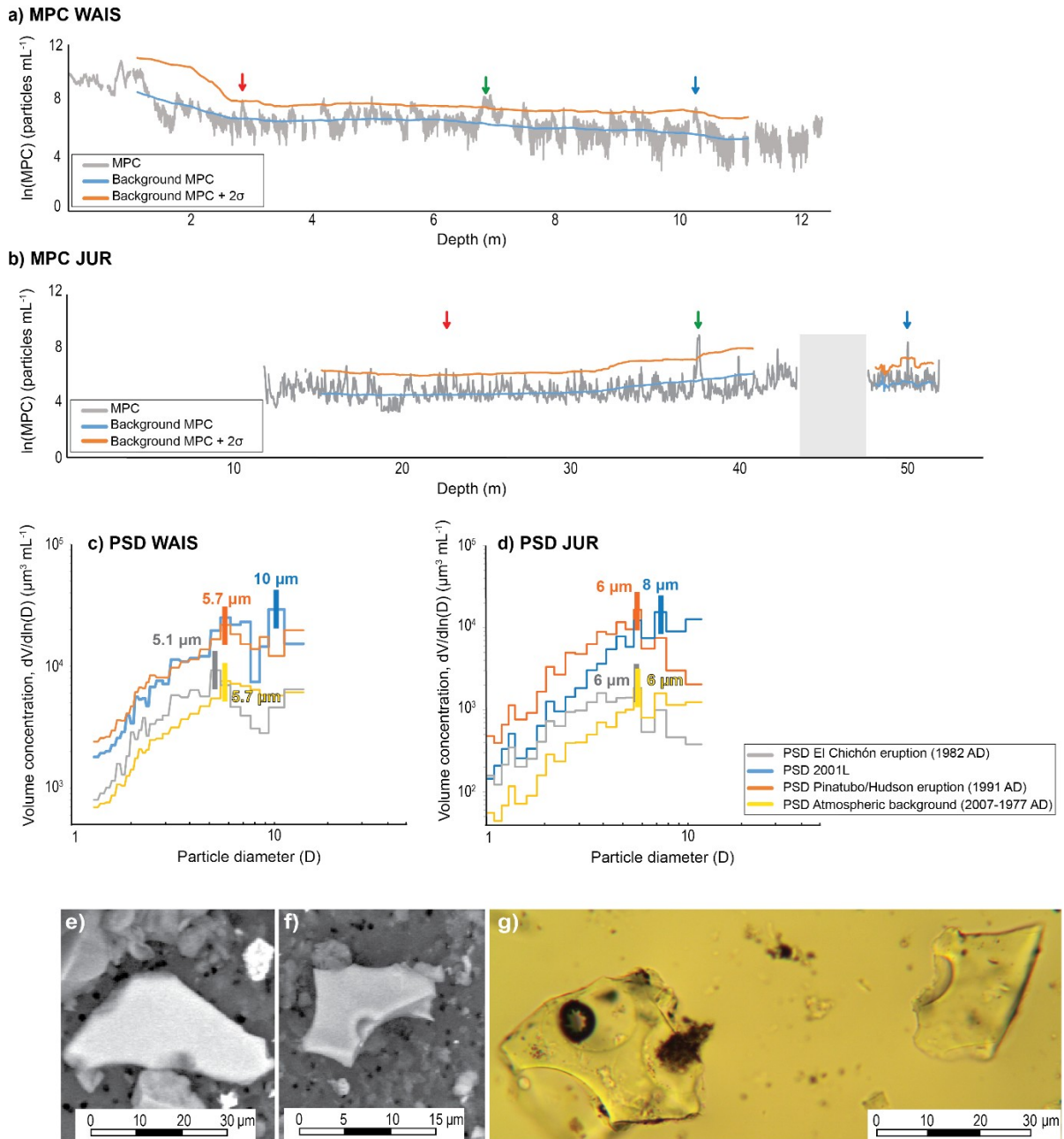
377 The volume concentration parameter (dV/dlnD) of insoluble dust was calculated in  
378 WAIS and in JUR for several particle diameters to obtain the particle size distribution (PSD)  
379 (Figure 6c and 6d). In the WAIS core, the background PSD (1977-2007 AD) presented a steady  
380 increase in concentration with increasing particle diameter (1.3-5.7 µm), followed by a constant  
381 decrease for the coarser particles (5.7-15 µm). Similar distributions were observed in the three  
382 targeted horizons, but with an additional increase in the coarsest particles (10-12 µm). Despite  
383 the similarities, the PSD for Pinatubo/Hudson (1991 AD) and 2001L exhibited considerably  
384 higher volume concentration values, up to four- times higher than the background, with PSDs  
385 that were completely detached from the background PSD. Likewise, the PSD for El Chichón  
386 exhibited higher than background volume concentration values in the finer particles (3.0-5.1  
387 µm). Additional discrepancies were observed in the mode particle diameter. Whilst similar mode  
388 diameters were obtained in the background (5.7 µm), Pinatubo/Hudson (5.7 µm) and El Chichón  
389 (5.1 µm), the 2001L presented a considerably higher mode particle diameter (10 µm).

390 In the JUR core, the background PSD (1977-2007 AD) presented a steady increase in the  
391 volume concentration with increasing particle diameter (1.0-6.0 µm), followed by a slight  
392 decrease for the coarser particles (8-12 µm). The three targeted horizons exhibited slightly  
393 different distributions. The PSD for El Chichón exhibited a distribution and volume  
394 concentration similar to the background. However, the El Chichón PSD presented a  
395 comparatively higher volume concentration in the finer particles (3.0-6.0 µm), not identified in  
396 the background PSD. The PSD for Pinatubo/Hudson and 2001L present similar distributions  
397 with volume concentrations up to an order of magnitude higher than the background. Despite  
398 their similarities, the PSD for Pinatubo/Hudson displays a sharp decrease after reaching its  
399 highest particle diameter (D) value at D=6 µm, while the PSD for 2001L reaches a steady  
400 volume concentration value after D=8 µm. The mode particle diameters for Pinatubo/Hudson  
401 (1991 AD) and El Chichón (1982 AD) matched the mode particle diameter of the background (6  
402 µm). Unlike the other targeted horizons, the 2001L presented a higher mode particle diameter (8  
403 µm).

#### 404 3.3.3 Microscopy analyses

405 Two filters containing insoluble particulate material from the 2001L of JUR were  
406 analysed for microparticle characterization (Figure 6e). Seventy particles were identified as  
407 cryptotephra shards with a mean size of  $19.28 \pm 8.73$  µm (sizes ranging from 7 to 47 µm).  
408 Similarly, two filters containing insoluble particulate matter from the 2001L of GOM were  
409 analysed. Ten particles were identified as cryptotephra shards (Figure 6f) with a mean size of

410  $12.9 \pm 3.9 \mu\text{m}$  (sizes ranging from 7 to 20  $\mu\text{m}$ ). Most of the cryptotephra shards identified in  
 411 both sites (JUR and GOM) were characterized by angular morphologies and concave features  
 412 (vesicles) without evidence of alteration or corrosion. The cryptotephra shards are cusped, platy  
 413 with sharp edges and few with open vesicles and some with butterfly shape. Microscope slides  
 414 from the 2001L of JUR show ten cryptotephra shards with a mean size of 21  $\mu\text{m}$  and presented  
 415 platy and cusped textures with round vesicles (Figure 6g).



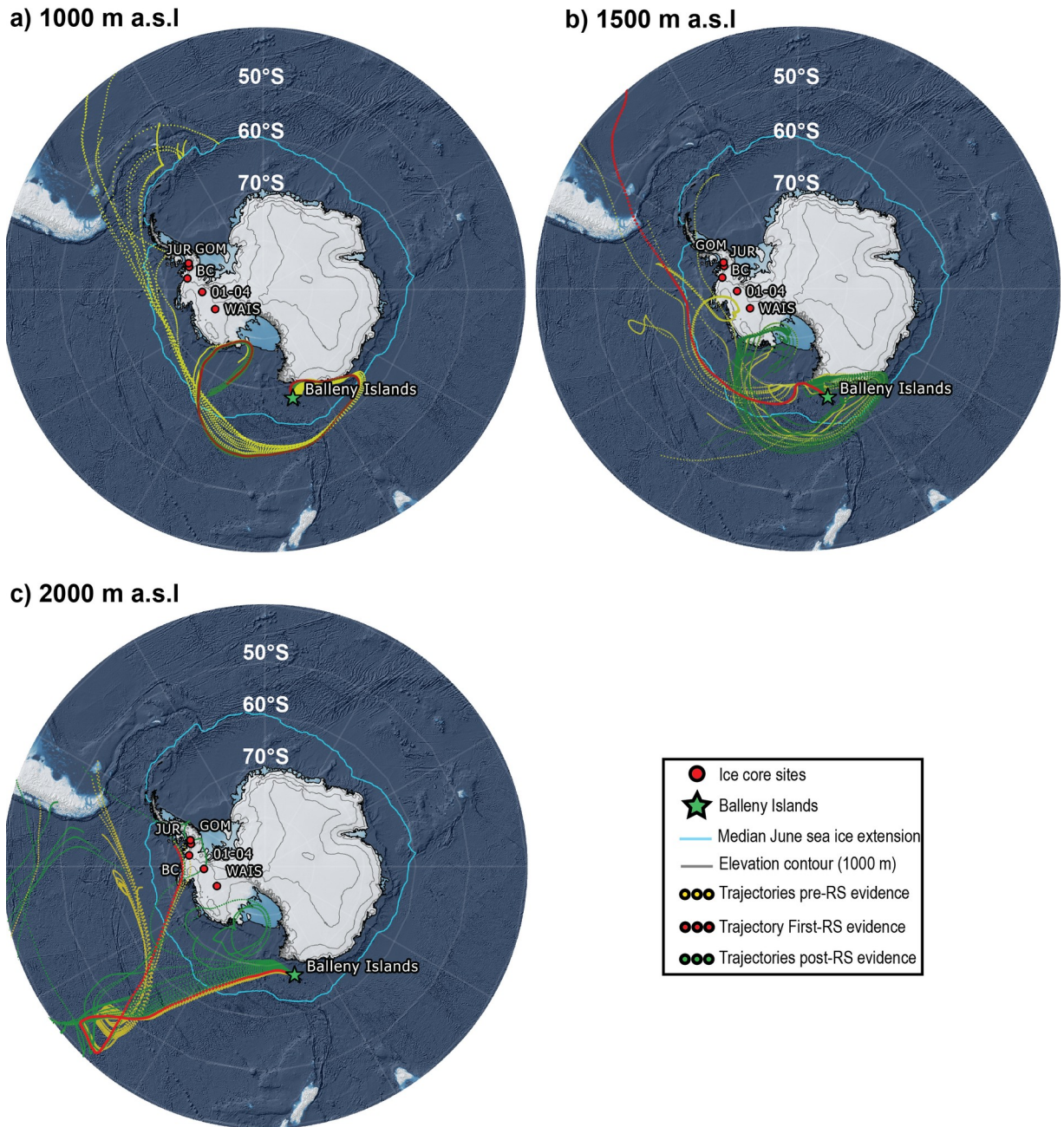
416

417 **Figure 6.** Microparticle analyses from WAIS and JUR ice cores. a) MPC for the depth interval  
 418 corresponding to the 1977-2007 AD period from the WAIS ice core. b) MPC for the depth  
 419 interval corresponding to the 1977-2007 AD period from the Jurassic ice core. Red arrows  
 420 indicate peaks above the detection threshold in the 2001 AD ice core layer. Green arrows

421 indicate peaks above the detection threshold in the 1994-1992 AD ice core layer. Blue arrows  
422 indicate peaks above the detection threshold in the 1984-1982 AD ice core layer. The grey band  
423 indicates a gap in the dust record. c) PSD curves from the WAIS ice core. d) PSD curves from  
424 the Jurassic ice core. e) and f) show SEM micrographs of cryptotephra shards identified in the  
425 2001 ice core layer from JUR and GOM ice cores respectively. g) Light microscope micrograph  
426 of cryptotephra shards identified in the 2001 AD ice core layer from Jurassic ice core.

### 427 3.4 Air mass trajectories

428 Forward trajectory analyses showed most of the air masses passing over the Balleny  
429 Islands on the 12<sup>th</sup> of June 2011 remained within the Southern Ocean for several days, mainly  
430 over the Somov, Ross, Amundsen and Bellingshausen Seas (Figure 7). Trajectories show air  
431 masses were predominantly travelling over the June sea-ice zone, with short periods (<72 hrs) of  
432 transit either over the Antarctic coast (<1000 m a.s.l.) or over the ice sheet (>1000 m a.s.l.). After  
433 leaving the Balleny Islands, all air masses moving at 1000 m a.s.l. transited over the Oates Coast,  
434 some of them reaching Saunders Coast in Marie Byrd Land (See Figure 1 for geographical  
435 references). A similar pattern is present in air masses moving at 1500 m a.s.l., where most  
436 trajectories transit over the same regions, but some also reach the Walgreen Coast, next to the  
437 Amundsen Sea Embayment. Trajectories over 2000 m a.s.l. present a different pattern with most  
438 trajectories moving north towards lower latitudes and only some of them travelling back south  
439 and over the ice sheet in Marie Byrd Land, Ellsworth Land and the southern Antarctic Peninsula.  
440 These trajectories passing over Ellsworth Land and the southern Antarctic Peninsula are the only  
441 trajectories reaching the ice core sites (GOM, JUR, BC, 01-4). These five trajectories represent  
442 the paths followed by air masses passing over the Balleny Islands at: 1200, 1300, 1400, 2300  
443 UTC on the 12<sup>th</sup> June 2011 and at 0200 UTC on the 13<sup>th</sup> June 2001. After leaving the Balleny  
444 Islands, four of these trajectories (1200, 1300, 1400 and 2300 UTC) were transported E-NE and  
445 then North, leaving the Southern Ocean and reaching ~ 43°S. Then they were transported back  
446 over the Southern Ocean southwards to the continent. The 0200 UTC trajectory remained within  
447 the June sea-ice zone and then over the ice sheet in Ellsworth Land and the southern Antarctic  
448 Peninsula. An additional cluster of five trajectories was identified passing near WAIS and 01-4  
449 ice core sites at 1500 m a.s.l. These trajectories were passing over the Balleny Islands between  
450 0800-1300 UTC on the 12<sup>th</sup> June 2001. After leaving the Balleny Islands they were transported  
451 over the June sea-ice zone of the Amundsen Sea and then reached the Walgreen Coast in the  
452 Amundsen Sea embayment.



453

454 **Figure 7.** Trajectories departing from Sturge Island on the 12<sup>th</sup> of June 2001 at three different  
 455 heights: a) 1000, b) 1500 and c) 2000 m a.s.l. Colour coded trajectories indicate if they passed  
 456 through Sturge Island before, during or after the first remote sensing evidence of an unusual  
 457 cloud formation. Median June sea ice-extension is based on 1980-2010 AD

458 **4 Discussion**

459 **4.1 Pinatubo/Hudson (1991 AD) and El Chichón (1982 AD) eruptions**

460 The 1994-1992 AD and 1984-1982 AD ice core layers are distinctive periods in the ice  
 461 core record. These intervals show strong similarities in the presence and consistency of  
 462 prominent summer peaks above the background variability in total sulphate concentration

463 ( $\text{SO}_4^{2-}$ ), Electrical Conductivity (EC) and Microparticle concentration (MPC). The levels of  $\text{SO}_4^{2-}$   
464 and MPC in the two are above the detection threshold, suggesting an additional input of  $\text{SO}_4^{2-}$   
465 and microparticles during these periods. In Antarctica, the 1994-1992 AD and 1984-1982 AD ice  
466 core layers have been linked to the well-documented eruptions of Mount Pinatubo/Cerro Hudson  
467 (1991 AD)(Cole-Dai & Mosley-Thompson, 1999; Zhang et al., 2002; Jiang et al., 2012;  
468 Plummer et al., 2012; Osipov et al., 2014; Schwanck et al., 2017; Thoen et al., 2018; Hoffmann  
469 et al., 2020) and El Chichón (1982 AD)(Kohno et al., 1999; Traufetter et al., 2004; Jiang et al.,  
470 2012; Plummer et al., 2012; Inoue et al., 2017; Thoen et al., 2018), the two volcanic eruptions  
471 with the greatest  $\text{SO}_2$  emissions worldwide of the 1977-2007 AD period (Shinohara, 2008).  
472 Therefore, we propose the excess of  $\text{SO}_4^{2-}$  and microparticles identified during these periods  
473 (1994-1992 AD & 1984-1982 AD) were also derived from the large low-latitude (mid-latitude)  
474 Pinatubo (Cerro Hudson) and El Chichón eruptions.

475 Subtle differences were identified between the signals of  $\text{SO}_4^{2-}$ , nss  $\text{SO}_4^{2-}$ , EC and MPC  
476 from the 1994-1992 AD and 1984-1982 AD ice core layers. The principal difference was  
477 associated with the magnitude of the  $\text{SO}_4^{2-}$ , nss  $\text{SO}_4^{2-}$ , EC and MPC peak(s) in each layer. Peaks  
478 in the 1994-1992 AD ice core layer were higher and more persistent, while peaks from the 1984-  
479 1982 AD ice layer were smaller or absent (nss $\text{SO}_4^{2-}$ -flux). These discrepancies are explained by  
480 differences in the volumetric emissions from each eruption, classified on the logarithmic scale of  
481 the Volcanic Explosivity Index (VEI). As VEI-6 (VEI-5), the Pinatubo (Cerro Hudson) eruption  
482 released at least  $10 \text{ km}^3$  ( $1 \text{ km}^3$ ) of particles and gases to the atmosphere, whilst the El Chichón  
483 VEI-5 eruption, ejected only  $1 \text{ km}^3$ . The difference in the scale of these two eruptions accounts  
484 for the different signal strengths observed in the 1994-1992 and 1984-1982 AD ice layers. Our  
485 results are consistent with observations from several Antarctic ice cores presenting a stronger  
486 signal for Pinatubo/Hudson and a weaker signal for El Chichón (Plummer et al., 2012; Inoue et  
487 al., 2017; Thoen et al., 2018).

488 The records identified for the Pinatubo/Hudson and El Chichón eruptions provide two  
489 examples of how different parameters measured in ice cores from the southern Antarctic  
490 Peninsula, Ellsworth Land and Marie Byrd Land can effectively record recent major low-latitude  
491 volcanic eruptions.

#### 492 4.2 The 2001 AD ice core horizon

493 In 2001, remote sensing observations from Sturge Island presented inconclusive evidence  
494 for recent volcanic activity in the Balleny Islands. Numerous lines of evidence from the ice core  
495 record provide independent evidence that a high-latitude volcanic eruption occurred at this time.

496 The 2001 ice core layer (2001L) presents some of the most striking features identified in  
497 the 1977-2007 AD period. In particular, this layer exhibited a prominent and synchronous  $\text{SO}_4^{2-}$ -  
498  $\text{EC} > 2\sigma$ -peak on each ice core analysed. Its presence in ice across Marie Byrd Land, Ellsworth  
499 Land and the southern Antarctic Peninsula, highlights it as a persistent regional feature. Even  
500 though the  $>2\sigma$  signal is only represented by a single data point in two ice core records ( $\text{SO}_4^{2-}$  in  
501 JUR and WAIS), its consistent presence across the region rules out the possibility of analytical  
502 outliers or sample contamination. The magnitude and regional distribution of the  $\text{SO}_4^{2-}$ - $\text{EC} > 2\sigma$ -  
503 peaks suggest it was caused by an exceptional input of sulphates to an extended area of the ice  
504 sheet during mid-2001. Further analyses of the MSA record showed the absence of peaks during  
505 the austral autumn/winter of 2001. Thus, demonstrating the  $\text{SO}_4^{2-}$ - $\text{EC} > 2\sigma$ -peak was not produced  
506 by increased austral autumn/winter marine biogenic productivity. The lack of evidence for a

507 biogenic source suggests the  $\text{SO}_4^{2-}$ > $2\sigma$ -peak identified in the 2001 ice core layer could only have  
508 been caused by inputs from a volcanic source. Detection of numerous cryptotephra glass shards  
509 in the mid-2001 AD ice core layer from the JUR and GOM ice cores provides direct evidence for  
510 a volcanic eruption. Combined with the observed MPC> $2\sigma$ -peak in WAIS and JUR for the  
511 2001L, this supports the assertion that the excess  $\text{SO}_4^{2-}$  is derived from a volcanic source. The  
512 elevated inputs of  $\text{SO}_4^{2-}$  & MPC recorded in 2001L are comparable to those observed in the  
513 1994-1992 AD and 1984-1982 AD ice core layers, attributed to Pinatubo/Hudson and El  
514 Chichón eruptions, respectively (section 4.1).

515 Results from Particle Size Distribution (PSD) analyses spatially constrain a possible  
516 source for the 2001 volcanic products. In particular, the PSD profile for the 2001 MPC> $2\sigma$ -peak  
517 presented a considerable increase in the volume and size of particles (mode diameter = 10  $\mu\text{m}$ ),  
518 compared with the background PSD (mode diameter = 5.7  $\mu\text{m}$ ). The coarser-than background  
519 PSD in 2001L suggest a more proximal volcanic source (Koffman et al., 2013) because coarser  
520 particles are unlikely to be transported large distances. Additionally, the spatial gradient  
521 identified in the volcanic sulphate flux suggests the transport and deposition of volcanic sulphate  
522 was from the Amundsen Sea sector towards the Bellingshausen Sea sector. Thus, establishing an  
523 eastward dispersion of the volcanic cloud. Results from the PSD and the net volcanic sulphate  
524 fluxes (VSF) are complemented by the synchronous deposition of the  $\text{SO}_4^{2-}$ , EC and MPC peaks  
525 that indicate rapid tropospheric transport and therefore also support a closer volcanic source  
526 (Koffman et al., 2017). Similarly, the angular texture of the cryptotephra suggest these glass  
527 shards were produced, transported and deposited within a short interval, without being altered by  
528 reworking or weathering processes.

529 To date, the Global Volcanic Program list of volcanic emissions only record two major  
530 volcanic events ( $\text{VEI} \geq 4$ ) for the 1998-2001 AD period. These events correspond to Shiveluch  
531 volcano in Russia (ongoing eruption since 1999 AD,  $\text{VEI}=4$ ) and to Ulawun volcano in Papua  
532 New Guinea (September 2000 AD,  $\text{VEI}=4$ ). Additionally, during the same period, there is only  
533 one confirmed major source of  $\text{SO}_2$  volcanic emissions, the Nyamuragira volcano in equatorial  
534 Africa (Shinohara, 2008). In the 1998-2001 AD period, the Nyamuragira volcano erupted three  
535 times: October 1998 AD, January 2000 AD and February 2001 AD. All these eruptions  
536 presenting a  $\text{VEI}=2$ . Despite the evidence of two major volcanic events and considerable  $\text{SO}_2$   
537 volcanic emissions from Nyamuragira during the 1998-2001 AD period, all these events  
538 occurred either in the equatorial region or in the northern hemisphere mid-latitudes. The distant  
539 location of these eruptions, their magnitude ( $\text{VEI} \leq 4$ ) and their timing cannot explain the  
540 synchronous  $\text{SO}_4^{2-}$ , EC and MPC peaks or the presence of cryptotephra shards in the 2001L.  
541 Thus, establishing a small to moderate Antarctic eruption as the potential source of volcanic  
542 products present in the 2001 ice core layer.

543 Mount Erebus has been volcanically active since 1972 AD and is the only volcano listed  
544 to have recorded volcanic activity in Antarctica between 1998-2001 AD. The eruptions recorded  
545 during this period were of Strombolian type and not exceeding  $\text{VEI}=2$ . There was a substantial  
546 increase in the number of eruptions per month during 1998 AD and 2000 AD. However, there  
547 was a sharp decrease in the number of eruptions after May 2000 AD, leading to the absence of  
548 eruptions between March 2001 and February 2002 (Global Volcanism Program, 2006, Global  
549 Volcanism Program, 2017). Despite the potential of Mount Erebus to be considered as the source  
550 to the volcanic signature in the 2001L, the relatively continuous emission from small eruptions  
551 would be represented in the ice core record as the background signal, rather than as prominent

552 peaks. Moreover, the proximity of Mount Erebus to the ice core sites would require a small to  
553 moderate eruption to have occurred in mid-2001. However, the lack of eruptions during this  
554 period rules out the possibility of Erebus as the source of volcanic products seen in the 2001 ice  
555 core layer. Although Mount Erebus is discarded as the volcanic source, a potential small to  
556 moderate Antarctic eruption is consistent with remote sensing observations from Sturge Island  
557 on the 12<sup>th</sup> of June 2001.

558 The analyses of air mass transport pathways provide key evidence linking remote sensing  
559 observations to the ice core record. Trajectory analyses confirm air parcels passing over Sturge  
560 Island at low elevations (1500 and 2000 m a.s.l) during the unusual cloud formation, were  
561 transported to the ice core sites in Ellsworth Land and southern Antarctic Peninsula within a  
562 week. The detection of a volcanic signal in the WAIS ice core, despite trajectories not passing  
563 directly over the ice core site, can be explained by the coarse resolution of the trajectory model  
564 (2.5 degrees lat.-long.), potential mixing with neighbouring air parcels (both vertically and  
565 horizontally), and/or trajectories reaching the site after the designated 10-day period. The air  
566 masses passing over Sturge Island on the 12<sup>th</sup> of June 2001, likely incorporated particles and  
567 chemical compounds from the eruption cloud then carried and deposited them over Marie Byrd  
568 Land, Ellsworth Land and the southern Antarctic Peninsula.

569 Results presented here are consistent with previous studies identifying the Balleny  
570 Islands as the source of earlier volcanic products preserved in the ice core record from Marie  
571 Byrd Land (Dunbar et al., 2003; Kurbatov et al., 2006; Koffman et al., 2013). In particular,  
572 Buckle Island is suggested as the source of three cryptotephra layers deposited on 1839 AD,  
573 1809 AD and 1804 AD (Kurbatov et al., 2006). The most recent of which was confirmed by  
574 historical records from sailors who observed a volcanic plume rising from Buckle Island in 1839  
575 AD (LeMasurier et al., 1990). This 1839 eruption was recognized in the WAIS ice core and  
576 characterized by the presence of cryptotephra in two horizons with elevated particle  
577 concentration and a considerable increase of the mode particle diameter ( $>10\ \mu\text{m}$ ) over the PSD  
578 background dust ( $5.1\ \mu\text{m}$ ) (Koffman et al., 2013). Likewise, several cryptotephra layers  
579 identified in the ice core record show that Antarctic eruptions typically increase the mode  
580 particle diameter ( $>6\ \mu\text{m}$ ) (Narcisi et al., 2010; Koffman et al., 2013) corresponding with  
581 elevated  $\text{SO}_4^{2-}$ -EC and MPC deposition. In addition, air mass trajectories are consistent with  
582 previous studies showing the absence of a 2001 Sturge Island eruption record in ice cores from  
583 the inland sites of Mount Johns and the Ellsworth Mountains in the West Antarctic ice sheet  
584 (Thoen et al., 2018; Hoffmann et al., 2020).

585 In summary, the ice core records, air mass trajectory analyses and remote sensing  
586 observations presented here provide strong evidence that a short-lived, small to moderate  
587 volcanic eruption took place on Sturge Island in mid-2001. Evidence suggests that volcanic  
588 products from this eruption were rapidly transported through the troposphere and deposited  
589 inland over Marie Byrd Land, Ellsworth Land and the southern Antarctic Peninsula. The  
590 deposition over the ice sheet produced a volcanically enriched layer that has been preserved in  
591 the ice core record.

592 The detection of this 2001 eruption demonstrates Sturge Island is an active volcano  
593 capable of producing small-moderate explosive events. It is possible that previous eruptions  
594 recognised in Antarctic ice core records and attributed to Buckle Island, could instead, have  
595 originated from Sturge Island. If true, Sturge Island could be at least as active as Buckle Island.  
596 Thus, suggesting a reinterpretation of the Balleny Island hot-spot dynamics (Green, 1992).

597 Additionally, the prominent and consistent volcanic signal identified in the 2001 ice core layers  
598 from Marie Byrd Land, Ellsworth Land and the southern Antarctic Peninsula highlight this ice  
599 core horizon as a new, XXI century, chronostratigraphic marker between the eruptions of  
600 Pinatubo/Hudson (1991 AD, VEI=6 and VEI=5) and Puyehue-Cordon Caulle (2011 AD,  
601 VEI=5). As such, the Sturge Island 2001 eruption provides a valuable volcanic horizon to date  
602 ice cores from the Amundsen and Bellingshausen Seas sectors.

603 The evidence presented in this work of a new XXI century volcanic horizon in West  
604 Antarctic ice cores supports the occurrence of a volcanic eruption in Sturge Island in 2001.  
605 Whilst, geochemical analyses of the cryptotephra shards would be required to unequivocally  
606 determine the Balleny Islands as the volcanic source, the evidence presented here is sufficiently  
607 robust to assign this cryptotephra layer in ice cores as a chronostratigraphic marker.

## 608 **5 Conclusions**

609 Antarctica is one of the most uncertainly active volcanic regions on Earth, with hundreds  
610 of volcanoes hidden beneath the ice sheet. New historical records of active volcanism in  
611 Antarctica provide valuable information to study how volcanic activity can shape the polar  
612 climate and its potential impacts on the cryosphere. A set of ice core records from Marie Byrd  
613 Land, Ellsworth Land and the southern Antarctic Peninsula have been analysed to validate  
614 previous inconclusive evidence of a 2001 volcanic eruption on Sturge Island, part of the Balleny  
615 Island chain. The 2001 ice core layer contains a regional input of sulphates and microparticles  
616 consistent with a volcanic source. Particle coarsening and in-phase deposition of volcanic  
617 products evidenced a small to moderate Antarctic eruption as the source and a rapid tropospheric  
618 dispersion as the transport mechanism. Air mass trajectory analyses proved air parcels passing  
619 over Sturge Island during the 2001 eruption were effectively transported, within a week, to the  
620 ice core sites.

621 The evidence presented here builds on previous inconclusive remote sensing observations  
622 to advocate Sturge Island as an active volcano with recent eruptive states. The regional extent of  
623 this volcanic event across several Antarctic ice core records highlights its potential as a  
624 chronostratigraphic marker to improve the accuracy of 21<sup>st</sup> century ice chronologies. Further  
625 research should be focused on performing geochemical analyses of the cryptotephra shards to  
626 unequivocally fingerprint the volcanic source.

## 627 **Acknowledgments**

628 We would like to thank Christine Lane from the Geography Department, University of  
629 Cambridge, for her help with cryptotephra shard identification. We would like to thank Professor  
630 Eric Wolff from the Earth Sciences Department, University of Cambridge, for his comments and  
631 suggestions during the final reviewing and editing of this draft. Also, we would like to thank the  
632 Ice core Lab staff from the British Antarctic Survey, for their help while processing the Jurassic  
633 ice core. This research was funded by CONICYT–Becas Chile and Cambridge Trust funding  
634 program for PhD studies. Grant number 72180432.

## 635 **Data Availability Statement**

636 Datasets for this research are available in these in-text data citation references: Thomas et  
637 al., 2008; Thomas et al., 2015; Mayewski and Dixon, 2005; Sigl et al., 2016. WAIS Divide  
638 datasets are available at National Snow and Ice Data Center (<https://nsidc.org/data/agdc/data->

639 wais-divide) and at the U.S. Antarctic Program Data Center (<https://www.usap-dc.org/>). Datasets  
 640 from the ITASE 01-4 ice core are available at NASA Earth Data Common Metadata repository  
 641 (<https://cmr.earthdata.nasa.gov/search/concepts/C1214591464-SCIOPS>). Datasets original to this  
 642 work will be available at the UK Polar Data Center (<https://www.bas.ac.uk/data/uk-pdc/>).

### 643 **Conflict of interest**

644 The authors declare that the research was conducted in the absence of any commercial or  
 645 financial relationships that could be construed as a potential conflict of interest.

### 646 **References**

- 647 Abram, N. J., Thomas, E. R., McConnell, J. R., Mulvaney, R., Bracegirdle, T. J., Sime, L. C., &  
 648 Aristarain, A. J. (2010). Ice core evidence for a 20th century decline of sea ice in the  
 649 Bellingshausen Sea, Antarctica. *Journal of Geophysical Research:*  
 650 *Atmospheres*, 115(D23).
- 651 Abram, N. J., Mulvaney, R., & Arrowsmith, C. (2011). Environmental signals in a highly  
 652 resolved ice core from James Ross Island, Antarctica. *Journal of Geophysical Research:*  
 653 *Atmospheres*, 116(D20).
- 654 Abram, N. J., Mulvaney, R., Wolff, E. W., Triest, J., Kipfstuhl, S., Trusel, L. D., Vimeux, F.,  
 655 Fleet, L., & Arrowsmith, C. (2013). Acceleration of snow melt in an Antarctic Peninsula  
 656 ice core during the twentieth century. *Nature Geoscience*, 6(5), 404–411.  
 657 <https://doi.org/10.1038/ngeo1787>
- 658 Aristarain, A. J., & Delmas, R. J. (1998). Ice record of a large eruption of Deception Island  
 659 Volcano (Antarctica) in the XVIIth century. *Journal of Volcanology and Geothermal*  
 660 *Research*, 80(1-2), 17-25.
- 661 Basile, I., Petit, J. R., Touron, S., Grousset, F. E., & Barkov, N. (2001). Volcanic layers in  
 662 Antarctic (Vostok) ice cores: Source identification and atmospheric implications. *Journal*  
 663 *of Geophysical Research: Atmospheres*, 106(D23), 31915-31931.
- 664 Bingham, R. G., & Siegert, M. J. (2009). Quantifying subglacial bed roughness in Antarctica:  
 665 implications for ice-sheet dynamics and history. *Quaternary Science Reviews*, 28(3-4),  
 666 223-236.
- 667 Breton, D. J., Koffman, B. G., Kurbatov, A. V., Kreutz, K. J., & Hamilton, G. S. (2012).  
 668 Quantifying signal dispersion in a hybrid ice core melting system. *Environmental science*  
 669 *& technology*, 46(21), 11922-11928.
- 670 Budner, D., & Cole-Dai, J. (2003). The number and magnitude of large explosive volcanic  
 671 eruptions between 904 and 1865 AD: Quantitative evidence from a new South Pole ice  
 672 core. *GEOPHYSICAL MONOGRAPH-AMERICAN GEOPHYSICAL UNION*, 139, 165-  
 673 176.
- 674 Castellano, E., Becagli, S., Jouzel, J., Migliori, A., Severi, M., Steffensen, J. P., Traversi, R., &  
 675 Udisti, R. (2004). Volcanic eruption frequency over the last 45 ky as recorded in Epica-  
 676 Dome C ice core (East Antarctica) and its relationship with climatic changes. *Global and*  
 677 *Planetary Change*, 42(1–4), 195–205. <https://doi.org/10.1016/j.gloplacha.2003.11.007>

- 678 Cole-Dai, J., Mosley-Thompson, E., & Thompson, L. G. (1997). Annually resolved southern  
679 hemisphere volcanic history from two Antarctic ice cores. *Journal of Geophysical*  
680 *Research: Atmospheres*, 102(D14), 16761-16771.
- 681 Cole-Dai, J., & Mosley-Thompson, E. (1999). The Pinatubo eruption in South Pole snow and its  
682 potential value to ice-core paleovolcanic records. *Annals of Glaciology*, 29, 99-105.
- 683 Cole-Dai, J., Mosley-Thompson, E., Wight, S. P., & Thompson, L. G. (2000). A 4100-year  
684 record of explosive volcanism from an East Antarctica ice core. *Journal of Geophysical*  
685 *Research: Atmospheres*, 105(D19), 24431-24441.
- 686 Cole-Dai, J. (2010). Volcanoes and climate. *Wiley Interdisciplinary Reviews: Climate*  
687 *Change*, 1(6), 824-839.
- 688 Criscitiello, A. S., Das, S. B., Evans, M. J., Frey, K. E., Conway, H., Joughin, I., Medley, B., &  
689 Steig, E. J. (2013). Ice sheet record of recent sea-ice behavior and polynya variability in  
690 the Amundsen Sea, West Antarctica. *Journal of Geophysical Research: Oceans*, 118(1),  
691 118–130. <https://doi.org/10.1029/2012jc008077>
- 692 Curran, M. A., van Ommen, T. D., Morgan, V. I., Phillips, K. L., & Palmer, A. S. (2003). Ice core  
693 evidence for Antarctic sea ice decline since the 1950s. *Science*, 302(5648), 1203-1206.
- 694 Dixon, D., Mayewski, P. A., Kaspari, S., Sneed, S., & Handley, M. (2004). A 200 year sub-  
695 annual record of sulfate in West Antarctica, from 16 ice cores. *Annals of Glaciology*, 39,  
696 545-556.
- 697 Draxler, R. R., & Hess, G. D. (1998). An overview of the HYSPLIT\_4 modelling system for  
698 trajectories. *Australian meteorological magazine*, 47(4), 295-308.
- 699 Dunbar, N. W., Zielinski, G. A., & Voisins, D. T. (2003). Tephra layers in the Siple Dome and  
700 Taylor Dome ice cores, Antarctica: Sources and correlations. *Journal of Geophysical*  
701 *Research: Solid Earth*, 108(B8).
- 702 Dunbar, N. W., & Kurbatov, A. V. (2011). Tephrochronology of the Siple Dome ice core, West  
703 Antarctica: correlations and sources. *Quaternary Science Reviews*, 30(13-14), 1602-1614.
- 704 de Vries, M. V. W., Bingham, R. G., & Hein, A. S. (2018). A new volcanic province: an  
705 inventory of subglacial volcanoes in West Antarctica. Geological Society, London,  
706 Special Publications, 461(1), 231-248.
- 707 Fujita, S., Parrenin, F., Severi, M., Motoyama, H., & Wolff, E. W. (2015). Volcanic  
708 synchronization of Dome Fuji and Dome C Antarctic deep ice cores over the past 216  
709 kyr. *Climate of the Past*, 11(10), 1395-1416.
- 710 Gautier, E., Savarino, J., Erbland, J., Lanciki, A., & Possenti, P. (2016). Variability of sulfate  
711 signal in ice core records based on five replicate cores. *Climate of the Past*, 12(1), 103-  
712 113.
- 713 Global Volcanism Program, 2001. Report on Sturge Island (Antarctica) (Wunderman, R.,  
714 ed.). *Bulletin of the Global Volcanism Network*, 26:5. Smithsonian Institution.  
715 <https://doi.org/10.5479/si.GVP.BGVN200105-390012>

- 716 Global Volcanism Program, 2006. Report on Erebus (Antarctica) (Wunderman, R., ed.). Bulletin  
717 of the Global Volcanism Network, 31:12. Smithsonian Institution.  
718 <https://doi.org/10.5479/si.GVP.BGVN200612-390020>.
- 719 Global Volcanism Program, 2017. Report on Erebus (Antarctica) (Crafford, A.E., and Venzke, E.,  
720 eds.). Bulletin of the Global Volcanism Network, 42:6. Smithsonian Institution.  
721 <https://doi.org/10.5479/si.GVP.BGVN201706-390020>.
- 722 Goodwin, B. P. (2013). *Recent Environmental Changes on the Antarctic Peninsula as Recorded*  
723 *in an ice core from the Bruce Plateau* (Doctoral dissertation, The Ohio State University).
- 724 Green, T. H. (1992). Petrology and geochemistry of basaltic rocks from the Balleny Is,  
725 Antarctica. *Australian Journal of Earth Sciences*, 39(5), 603-617.
- 726 Hoffmann, K., Fernandoy, F., Meyer, H., Thomas, E. R., Aliaga, M., Tetzner, D., Freitag, J.,  
727 Opel, T., Arigony-Neto, J., Göbel, C. F., Jaña, R., Rodríguez Oroz, D., Tuckwell, R.,  
728 Ludlow, E., McConnell, J. R., & Schneider, C. (2020). Stable water isotopes and  
729 accumulation rates in the Union Glacier region, Ellsworth Mountains, West Antarctica,  
730 over the last 35 years. *The Cryosphere*, 14(3), 881–904. [https://doi.org/10.5194/tc-14-](https://doi.org/10.5194/tc-14-881-2020)  
731 [881-2020](https://doi.org/10.5194/tc-14-881-2020)
- 732 Hund, A. J. (Ed.). (2014). *Antarctica and the Arctic Circle: A Geographic Encyclopedia of the*  
733 *Earth's Polar Regions* [2 volumes]. ABC-CLIO.
- 734 Inoue, M., Curran, M. A., Moy, A. D., van Ommen, T. D., Fraser, A. D., Phillips, H. E., &  
735 Goodwin, I. D. (2017). A glaciochemical study of the 120 m ice core from Mill Island,  
736 East Antarctica. *Climate of the Past*, 13(5), 437-453.
- 737 Jiang, S., Cole-Dai, J., Li, Y., Ferris, D. G., Ma, H., An, C., Shi, G., & Sun, B. (2012). A detailed  
738 2840 year record of explosive volcanism in a shallow ice core from Dome A, East  
739 Antarctica. *Journal of Glaciology*, 58(207), 65–75. <https://doi.org/10.3189/2012jog11j138>
- 740 JIANKANG, H., ZICHU, X., JIAHONG, W., JIANCHENG, K., & GUOCAI, Z. (1999). Mass  
741 balance study on Collins Ice Cap, King George Island, Antarctica: spatial and temporal  
742 variations. *IAHS-AISH publication*, 209-215.
- 743 Kittleman, L. R. (1979). Tephra. *Scientific American*, 241(6), 160-177.
- 744 Koffman, B. G., Kreutz, K. J., Kurbatov, A. V., & Dunbar, N. W. (2013). Impact of known local  
745 and tropical volcanic eruptions of the past millennium on the WAIS Divide microparticle  
746 record. *Geophysical research letters*, 40(17), 4712-4716.
- 747 Koffman, B. G., Kreutz, K. J., Breton, D. J., Kane, E. J., Winski, D. A., Birkel, S. D., Kurbatov,  
748 A. V., & Handley, M. J. (2014). Centennial-scale variability of the Southern Hemisphere  
749 westerly wind belt in the eastern Pacific over the past two millennia. *Climate of the Past*,  
750 10(3), 1125–1144. <https://doi.org/10.5194/cp-10-1125-2014>
- 751 Koffman, B. G., Dowd, E. G., Osterberg, E. C., Ferris, D. G., Hartman, L. H., Wheatley, S. D.,  
752 Kurbatov, A. V., Wong, G. J., Markle, B. R., Dunbar, N. W., Kreutz, K. J., & Yates, M.  
753 (2017). Rapid transport of ash and sulfate from the 2011 Puyehue-Cordón Caulle (Chile)  
754 eruption to West Antarctica. *Journal of Geophysical Research: Atmospheres*, 122(16),  
755 8908–8920. <https://doi.org/10.1002/2017jd026893>

- 756 KOHNO, M., FUJII, Y., KUSAKABE, M., & FUKUOKA, T. (1999). The last 300-year volcanic  
757 signals recorded in an ice core from site H15, Antarctica. *Journal of the Japanese Society*  
758 *of Snow and Ice*, 61(1), 13-24.
- 759 Kreutz, K. J., & Mayewski, P. A. (1999). Spatial variability of Antarctic surface snow  
760 glaciochemistry: implications for palaeoatmospheric circulation  
761 reconstructions. *Antarctic Science*, 11(1), 105-118.
- 762 Kreutz, K. J., Kurbatov, A. V., Wells, M., & Mayewski, P. A. (2011). COLLABORATIVE  
763 RESEARCH: Microparticle/tephra analysis of the WAIS Divide ice core.
- 764 Kreutz, K. et al. (2015) "WAIS Divide Microparticle Concentration and Size Distribution, 0-  
765 2400 ka" U.S. Antarctic Program (USAP) Data Center. doi:  
766 <https://doi.org/10.7265/N5KK98QZ>.
- 767 Kurbatov, A. V., Zielinski, G. A., Dunbar, N. W., Mayewski, P. A., Meyerson, E. A., Sneed, S. B.,  
768 & Taylor, K. C. (2006). A 12,000 year record of explosive volcanism in the Siple Dome  
769 Ice Core, West Antarctica. *Journal of Geophysical Research: Atmospheres*, 111(D12).
- 770 Lee, J. E., Brook, E. J., Bertler, N. A. N., Buizert, C., Baisden, T., Blunier, T., Ciobanu, V. G.,  
771 Conway, H., Dahl-Jensen, D., Fudge, T. J., Hindmarsh, R., Keller, E. D., Parrenin, F.,  
772 Severinghaus, J. P., Vallelonga, P., Waddington, E. D., & Winstrup, M. (2020). An 83  
773 000-year-old ice core from Roosevelt Island, Ross Sea, Antarctica. *Climate of the Past*,  
774 16(5), 1691–1713. <https://doi.org/10.5194/cp-16-1691-2020>
- 775 Legrand, M., & Mayewski, P. (1997). Glaciochemistry of polar ice cores: A review. *Reviews of*  
776 *geophysics*, 35(3), 219-243.
- 777 LeMasurier, W. E., Thomson, J. W., Baker, P. E., Kyle, P. R., Rowley, P. D., Smellie, J. L., &  
778 Verwoerd, W. J. (1990). *Volcanoes of the Antarctic plate and Southern Ocean* (Vol. 48).  
779 American Geophysical Union.
- 780 Li, C., Xiao, C., Hou, S., Ren, J., Ding, M., & Guo, R. (2012). Dating a 109.9 m ice core from  
781 Dome A (East Antarctica) with volcanic records and a firn densification model. *Science*  
782 *China Earth Sciences*, 55(8), 1280-1288.
- 783 Maupetit, F., & Delmas, R. J. (1992). Chemical composition of falling snow at Dumont d'Urville,  
784 Antarctica. *Journal of atmospheric chemistry*, 14(1-4), 31-42.
- 785 Mayewski, P. A. and D. A. Dixon. 2005. US International Trans Antarctic Scientific Expedition  
786 (US ITASE) glaciochemical data. Boulder, CO, USA: National Snow and Ice Data  
787 Center. Digital media.
- 788 Mulvaney, R., Abram, N. J., Hindmarsh, R. C. A., Arrowsmith, C., Fleet, L., Triest, J., Sime, L.  
789 C., Alemany, O., & Foord, S. (2012). Recent Antarctic Peninsula warming relative to  
790 Holocene climate and ice-shelf history. *Nature*, 489(7414), 141–144.  
791 <https://doi.org/10.1038/nature11391>
- 792 Mulvaney, R. (2013). ICE CORE METHODS | Conductivity Studies. In *Encyclopedia of*  
793 *Quaternary Science* (pp. 319–325). Elsevier. [https://doi.org/10.1016/b978-0-444-53643-](https://doi.org/10.1016/b978-0-444-53643-3.00311-3)  
794 [3.00311-3](https://doi.org/10.1016/b978-0-444-53643-3.00311-3)
- 795 Narcisi, B., Petit, J. R., Delmonte, B., Basile-Doelsch, I., & Maggi, V. (2005). Characteristics  
796 and sources of tephra layers in the EPICA-Dome C ice record (East Antarctica):

- 797 implications for past atmospheric circulation and ice core stratigraphic correlations. *Earth*  
798 *and Planetary Science Letters*, 239(3-4), 253-265.
- 799 Narcisi, B., Petit, J. R., & Delmonte, B. (2010). Extended East Antarctic ice-core  
800 tephrostratigraphy. *Quaternary Science Reviews*, 29(1-2), 21-27.
- 801 Narcisi, B., Petit, J. R., Delmonte, B., Scarchilli, C., & Stenni, B. (2012). A 16,000-yr tephra  
802 framework for the Antarctic ice sheet: a contribution from the new Talos Dome  
803 core. *Quaternary Science Reviews*, 49, 52-63.
- 804 Narcisi, B., Petit, J. R., Langone, A., & Stenni, B. (2016). A new Eemian record of Antarctic  
805 tephra layers retrieved from the Talos Dome ice core (Northern Victoria Land). *Global*  
806 *and planetary Change*, 137, 69-78.
- 807 Narcisi, B., Petit, J. R., Delmonte, B., Batanova, V., & Savarino, J. (2019). Multiple sources for  
808 tephra from AD 1259 volcanic signal in Antarctic ice cores. *Quaternary Science*  
809 *Reviews*, 210, 164-174.
- 810 Nardin, R., Amore, A., Becagli, S., Caiazza, L., Frezzotti, M., Severi, M., Stenni, B., & Traversi,  
811 R. (2020). Volcanic Fluxes Over the Last Millennium as Recorded in the Gv7 Ice Core  
812 (Northern Victoria Land, Antarctica). *Geosciences*, 10(1), 38.  
813 <https://doi.org/10.3390/geosciences10010038>
- 814 Osipov, E. Y., Khodzher, T. V., Golobokova, L. P., Onischuk, N. A., Lipenkov, V. Y., Ekaykin, A.  
815 A., Shibaev, Y. A., & Osipova, O. P. (2014). High-resolution 900 year volcanic and  
816 climatic record from the Vostok area, East Antarctica. *The Cryosphere*, 8(3), 843–851.  
817 <https://doi.org/10.5194/tc-8-843-2014>
- 818 Palais, J. M. (1985). Particle morphology, composition and associated ice chemistry of tephra  
819 layers in the Byrd ice core: Evidence for hydrovolcanic eruptions. *Annals of*  
820 *glaciology*, 7, 42-48.
- 821 Parrenin, F., Barker, S., Blunier, T., Chappellaz, J., Jouzel, J., Landais, A., Masson-Delmotte, V.,  
822 Schwander, J., & Veres, D. (2012). On the gas-ice depth difference ( $\Delta$ depth) along the  
823 EPICA Dome C ice core. *Climate of the Past*, 8(4), 1239–1255.  
824 <https://doi.org/10.5194/cp-8-1239-2012>
- 825 Patrick, M. R., & Smellie, J. L. (2013). Synthesis A spaceborne inventory of volcanic activity in  
826 Antarctica and southern oceans, 2000-10. *Antarctic Science*, 25(4), 475.
- 827 Plummer, C. T., Curran, M. A. J., van Ommen, T. D., Rasmussen, S. O., Moy, A. D., Vance, T.  
828 R., Clausen, H. B., Vinther, B. M., & Mayewski, P. A. (2012). An independently dated  
829 2000-yr volcanic record from Law Dome, East Antarctica, including a new perspective  
830 on the dating of the 1450s CE eruption of Kuwae, Vanuatu. *Climate of the Past*, 8(6),  
831 1929–1940. <https://doi.org/10.5194/cp-8-1929-2012>
- 832 Ren, J., Li, C., Hou, S., Xiao, C., Qin, D., Li, Y., & Ding, M. (2010). A 2680 year volcanic  
833 record from the DT-401 East Antarctic ice core. *Journal of Geophysical Research:*  
834 *Atmospheres*, 115(D11).
- 835 Robock, A. (2000). Volcanic eruptions and climate. *Reviews of geophysics*, 38(2), 191-219.

- 836 Röthlisberger, R., Bigler, M., Hutterli, M., Sommer, S., Stauffer, B., Junghans, H. G., &  
837 Wagenbach, D. (2000). Technique for continuous high-resolution analysis of trace  
838 substances in firn and ice cores. *Environmental Science & Technology*, 34(2), 338-342.
- 839 Ruth, U., Wagenbach, D., Steffensen, J. P., & Bigler, M. (2003). Continuous record of  
840 microparticle concentration and size distribution in the central Greenland NGRIP ice core  
841 during the last glacial period. *Journal of Geophysical Research: Atmospheres*, 108(D3).
- 842 Schwanck, F., Simões, J. C., Handley, M., Mayewski, P. A., Auger, J. D., Bernardo, R. T., &  
843 Aquino, F. E. (2017). A 125-year record of climate and chemistry variability at the Pine  
844 Island Glacier ice divide, Antarctica. *The Cryosphere*, 11(4), 1537-1552.
- 845 Severi, M., Udisti, R., Becagli, S., Stenni, B., & Traversi, R. (2012). Volcanic synchronisation of  
846 the EPICA-DC and TALDICE ice cores for the last 42 kyr BP. *Climate of the Past*, 8(2),  
847 509-517.
- 848 Shinohara, H. (2008). Excess degassing from volcanoes and its role on eruptive and intrusive  
849 activity. *Reviews of Geophysics*, 46(4).
- 850 Sigl, M., McConnell, J. R., Toohey, M., Curran, M., Das, S. B., Edwards, R., Isaksson, E.,  
851 Kawamura, K., Kipfstuhl, S., Krüger, K., Layman, L., Maselli, O. J., Motizuki, Y.,  
852 Motoyama, H., Pasteris, D. R., & Severi, M. (2014). Insights from Antarctica on volcanic  
853 forcing during the Common Era. *Nature Climate Change*, 4(8), 693–697.  
854 <https://doi.org/10.1038/nclimate2293>
- 855 Sigl, M., Fudge, T. J., Winstrup, M., Cole-Dai, J., Ferris, D., McConnell, J. R., Taylor, K. C.,  
856 Welten, K. C., Woodruff, T. E., Adolphi, F., Bisiaux, M., Brook, E. J., Buizert, C., Caffee,  
857 M. W., Dunbar, N. W., Edwards, R., Geng, L., Iverson, N., Koffman, B., ... Sowers, T. A.  
858 (2016). The WAIS Divide deep ice core WD2014 chronology – Part 2: Annual-layer  
859 counting (0–31 ka BP). *Climate of the Past*, 12(3), 769–786. [https://doi.org/10.5194/cp-](https://doi.org/10.5194/cp-12-769-2016)  
860 [12-769-2016](https://doi.org/10.5194/cp-12-769-2016)
- 861 Stein, A. F., Draxler, R. R., Rolph, G. D., Stunder, B. J., Cohen, M. D., & Ngan, F. (2015).  
862 NOAA's HYSPLIT atmospheric transport and dispersion modeling system. *Bulletin of*  
863 *the American Meteorological Society*, 96(12), 2059-2077.
- 864 Tetzner, D., Thomas, E. R., Allen, C. S., & Wolff, E. W. (2021). A Refined Method to Analyze  
865 Insoluble Particulate Matter in Ice Cores, and Its Application to Diatom Sampling in the  
866 Antarctic Peninsula. *Frontiers in Earth Science*, 9, 20.
- 867 Thoen, I. U., Simões, J. C., Lindau, F. G. L., & Sneed, S. B. (2018). Ionic content in an ice core  
868 from the West Antarctic Ice Sheet: 1882-2008 AD. *Brazilian Journal of Geology*, 48(4),  
869 853-865.
- 870 Thomas, E. R., Marshall, G. J., & McConnell, J. R. (2008). A doubling in snow accumulation in  
871 the western Antarctic Peninsula since 1850. *Geophysical research letters*, 35(1).
- 872 Thomas, E. R., Hosking, J. S., Tuckwell, R. R., Warren, R. A., & Ludlow, E. C. (2015).  
873 Twentieth century increase in snowfall in coastal West Antarctica. *Geophysical Research*  
874 *Letters*, 42(21), 9387-9393.
- 875 Thomas, E. R., & Abram, N. J. (2016). Ice core reconstruction of sea ice change in the  
876 Amundsen–Ross Seas since 1702 AD. *Geophysical Research Letters*, 43(10), 5309-5317.

- 877 Traufetter, F., Oerter, H., Fischer, H., Weller, R., & Miller, H. (2004). Spatio-temporal variability  
878 in volcanic sulphate deposition over the past 2 kyr in snow pits and firn cores from  
879 Amundsenisen, Antarctica. *Journal of Glaciology*, 50(168), 137-146.
- 880 Traversi, R., Becagli, S., Castellano, E., Migliori, A., Severi, M., & Udisti, R. (2002). High-  
881 resolution fast ion chromatography (FIC) measurements of chloride, nitrate and sulphate  
882 along the EPICA Dome C ice core. *Annals of Glaciology*, 35, 291-298.
- 883 Udisti, R., Becagli, S., Castellano, E., Mulvaney, R., Schwander, J., Torcini, S., & Wolff, E.  
884 (2000). Holocene electrical and chemical measurements from the EPICA–Dome C ice  
885 core. *Annals of Glaciology*, 30, 20-26.
- 886 Vogel, S. W., Tulaczyk, S., Carter, S., Renne, P., Turrin, B., & Grunow, A. (2006). Geologic  
887 constraints on the existence and distribution of West Antarctic subglacial  
888 volcanism. *Geophysical research letters*, 33(23).
- 889 Wagenbach, D., Ducroz, F., Mulvaney, R., Keck, L., Minikin, A., Legrand, M., Hall, J. S., &  
890 Wolff, E. W. (1998). Sea-salt aerosol in coastal Antarctic regions. *Journal of Geophysical*  
891 *Research: Atmospheres*, 103(D9), 10961–10974. <https://doi.org/10.1029/97jd01804>
- 892 Zhang, M. J., Li, Z. Q., Xiao, C. D., Qin, D. H., Yang, H. A., Kang, J. C., & Li, J. (2002). A  
893 continuous 250-year record of volcanic activity from Princess Elizabeth Land, East  
894 Antarctica. *Antarctic Science*, 14(1), 55.  
895